ASTROBIOLOGY
Volume 17, Number 1, 2017

DOI: 10.1089/ast.2016.1524

Low-Temperature Alkaline pH Hydrolysis of Oxygen-Free Titan Tholins: Carbonates' Impact

Coralie Brassé,[1] Arnaud Buch,[2] Patrice Coll,[1] and François Raulin[1]

Abstract

Titan, the largest moon of Saturn, is one of the key planetary objects in the field of exobiology. Its dense, nitrogen-rich atmosphere is the site of important organic chemistry. This paper focuses on the organic aerosols produced in Titan's atmosphere that play an important role in atmospheric and surface processes and in organic chemistry as it applies to exobiological interests. To produce reliable laboratory analogues of these aerosols, we developed, tested, and optimized a device for the synthesis of clean tholins. The potential chemical evolution of Titan aerosols at Titan's surface has been studied, in particular, the possible interaction between aerosols and putative ammonia-water cryomagma. Modeling of the formation of Saturn's atmosphere has permitted the characterization of a composition of salts in the subsurface ocean and cryolava. From this new and original chemical composition, a laboratory study of several hydrolyses of tholins was carried out. The results obtained show the formation of many organic compounds, among them, species identified only in the presence of salts. In addition, a list of potential precursors of these compounds was established, which could provide a database for research of the chemical composition of tholins and/or aerosols of Titan. Key Words: Titan tholins—Titan aerosols—Hydrolysis—Carbonates—Titan's surface. Astrobiology 17, 8–26.

1. Introduction

The largest moon of Saturn, Titan, is known for being the only planetary body in the Solar System that possesses a dense atmosphere comparable to that of Earth. It is essentially constituted of molecular nitrogen (varying from 95.0% to 98.4% with altitude) with a noticeable fraction of methane (varying from 5.00% to 1.48% with altitude). Other constituents have been detected at trace levels such as, in the stratosphere, hydrocarbons (all C_2 hydrocarbons, propane, propene, methylacetylene, diacetylene, benzene), nitriles (cyanogen, cyanoacetylene, hydrogen cyanide, acetonitrile, dicyanoacetylene), molecular hydrogen, carbon monoxide, carbon dioxide, water vapor, and argon (Samuelson *et al.*, 1983, 1997; Coustenis *et al.*, 1998, 2010; Marten *et al.*, 2002; Flasar *et al.*, 2005; Niemann *et al.*, 2005, 2010; Waite *et al.*, 2005; Nixon *et al.*, 2013). Several other compounds have also been detected in the ionosphere, in particular, negatively charged massive molecules (Waite *et al.*, 2007).

Titan's atmospheric composition is driven by the coupled chemistry of N_2 and CH_4 (Raulin *et al.*, 2012, and references therein). The complex organic chemistry occurring in this atmosphere is initiated in the ionosphere and involves large negative ions (Waite *et al.*, 2007). The dissociation of methane induced by photons with wavelengths lower than 150 nm provides CH, CH_2, and CH_3 radicals. The dissociation of dinitrogen is generated by photons with wavelengths lower than 100 nm and by energetic particles from Saturn's magnetosphere. Then the resulting products chemically evolve, coagulate, and/or condense. This evolution yields more complex compounds up to the production of macromolecular organic particles, forming Titan's haze. Those complex organic aerosols provide the characteristic orange-brown color of Titan in the visible spectral range. They also play an important role in radiative transfer models (McKay *et al.*, 1989, 1991), as well as in the composition and properties of the atmosphere of Titan. And they may interact chemically with geological features present on the surface and affect the chemical composition of the satellite's exterior. With the Cassini-Huygens mission, in particular the Synthetic Aperture Radar (SAR) and the Visual and Infrared Mapping Spectrometer (VIMS) images, the surface of Titan has been revealed to be geologically complex and diversified (Elachi *et al.*, 2005; McCord *et al.*, 2006). Although several large plains remain unknown (Lopes *et al.*, 2010), many geological features present on Earth have been observed on Titan's

[1]Laboratoire Interuniversitaire des Systèmes Atmosphériques (LISA), UMR CNRS 7583, Université Paris Est Créteil et Université Paris Diderot, Institut Pierre Simon Laplace, C.M.C., Créteil, France.
[2]Laboratoire de Génie des Procédés et Matériaux (LGPM), Ecole Centrale Paris, Chatenay-Malabry, France.

surface, such as volcanoes, craters, sand dunes, lakes, seas, and mountains. These geological structures are constantly covered by solid organic aerosols deposited by precipitation or dry deposition. For those reasons, it is important to understand how Titan's aerosols chemically evolve once deposited at Titan's surface in order to determine whether astrobiologically interesting molecules could be formed.

In this paper, we focus on the likely cryovolcanic area potentially identified on Titan's surface (Barnes *et al.*, 2005, 2006; Lopes *et al.*, 2007, 2010, 2013; Nelson *et al.*, 2009; Soderblom *et al.*, 2009; Wall *et al.*, 2009). Cryovolcanism refers to the eruption of materials of low density and low melting point, which constitute part of Titan's interior (as the plausible subsurface ocean). The presence of cryovolcanic processes has been suggested by Lorenz (1993) and Lorenz and Lunine (1996). It has been tentatively observed after Cassini's arrival to the Saturn system. In particular, the SAR and VIMS data have provided images from the surface that highlight potential cryovolcanic activity. With VIMS data, it is possible to detect surface changes that could indicate a currently active cryovolcanism on Titan. But the interpretation of those data is still controversial since the SAR images alone lead to a different conclusion, compared to those derived from both VIMS and SAR data. Lopes *et al.* (2007) observed signs of cryovolcanism flow in the Ganesa region on Titan via SAR data processing. Also, it has been pointed out that cryovolcanism could be a minor geological process with sporadic activity (Tobie *et al.*, 2006; Mitri *et al.*, 2008). Indeed, SAR data show that the cryovolcanism area would only represent a tiny part of the surface: roughly 1.2% between 90°N and 90°S (an area corresponding to 20% of the total titanian surface). Nevertheless, plains cover a large part of the surface of Titan, but their nature is still unclear. If their origin is cryovolcanic, it could suggest that cryovolcanism would have been involved at one moment in the history of Titan (Lopes *et al.*, 2010, 2013). Lopes *et al.* (2010, 2013) proposed that most of the cryovolcanic features are located from 30°S to 60°N (Table 1). Within this location, two regions seem to be good candidates for cryovolcanism, in particular because of the presence of caldera-like structures and potential surface changes, Hotei Regio and Tui Regio (Barnes *et al.*, 2005, 2006; Nelson *et al.*, 2009; Soderblom *et al.*, 2009; Wall *et al.*, 2009; Lopes *et al.*, 2010, 2013), which do not exclude the assumption of the sedimentary alternative.

Lopes *et al.* (2007, 2010, 2013) also suggested that Ganesa Macula, which was first interpreted as a volcanic dome (Elachi *et al.*, 2005; Lopes *et al.*, 2007), could be a cryovolcanism region. Indeed, recent studies have shown that the features of Ganesa do not fit with a volcanic dome (Kirk *et al.*, 2008; Stiles *et al.*, 2009). Furthermore, by combining RADAR and VIMS data, Lopes *et al.* (2011) explained that Ganesa Macula could not be a cryovolcanic area. A similar interpretation has been made for the Winia Fluctus region. The Sotra Facula region has also been suggested as a cryovolcanic feature candidate via SAR (Lopes *et al.*, 2010) and RADAR stereogrammetry (Kirk *et al.*, 2008). This region could also be partially covered by dunes, which would imply that the cryovolcanic features are relatively young (Lopes *et al.*, 2010). This region includes the sites named Mohini Fluctus, Sotra Patera, Doom Mons, and Erebor Mons. It has been suggested that these four areas have been shaped by cryovolcanic processes (Lopes *et al.*, 2010). Rohe Fluctus and Ara Fluctus are also considered potential candidates for cryovolcanism since they show caldera-like depressions associated with flow features as is the case for Mohini Fluctus (Lopes *et al.*, 2007, 2013). Wall *et al.* (2009) showed that both Western Xanadu and Hotei Arcus regions exhibit variable infrared brightness that could be evidence of active cryovolcanoes. Nevertheless, Soderblom *et al.* (2009) questioned the approach used to extract the reflectance data, and they take this hypothesis with caution. Sotin *et al.* (2005) interpreted that the region Tortola Facula (also known as Sotra Patera) from VIMS data could be a cryovolcanic area, while Sotin *et al.* (2010) and Hayes *et al.* (2008) interpreted this region to be ''hummocky and mountainous terrain units.'' Lopes *et al.* (2011) also concluded that this region would have other origins than cryovolcanism.

In summary, Ganesa Macula and Winia Fluctus could not be cryovolcanic areas. For Tui Regio and Western Xanadu, the cryovolcanic interpretation remains uncertain, while Sotra Facula and Hotei Regio could be the strongest candidates for cryovolcanic regions (Lopes *et al.*, 2011, 2013). Nevertheless, the low resolution of the data sets is a real issue, so several cryovolcanic features may not have been identified yet.

Although its composition remains unknown, it is often suggested that the cryomagma could be a mixture of water-ammonia (Grasset *et al.*, 2000; Tobie *et al.*, 2005) and may also include methanol (Lopes *et al.*, 2007). Mitri *et al.* (2008) made the assumption that the composition of the cryomagma could be connected to the composition of the internal ocean. Models predict the presence of a water-ammonia ocean located between a low-pressure water ice layer and a high-pressure water ice layer (Tobie *et al.*, 2005, 2012). The possibility of such an internal ocean is supported by several observations such as the changing of Titan's rotation (Lorenz *et al.*, 2008) or the uncommon Schumann resonance in Titan's atmosphere (Béghin *et al.*, 2012). Mitri *et al.* (2008) showed that the putative water-ammonia cryomagma could slowly reach the surface through cracks at the base of the low-pressure water ice layer. The fraction of

Table 1. Candidate Cryovolcanic Features on Titan (Adapted from Lopes *et al.*, 2013)

Not Cryovolcanic	Possibly Cryovolcanic	Strongest Candidates
Ganesa Macula (87.3°W, 50.0°N)	Ara Fluctus (118.4°W, 39.8°N)	Sotra Patera (40.0°W, 14.5°S)
Tortola Facula (143.1°W, 8.8°N)	Western Xanadu (140°W, 10°S)	Doom Mons (40.4°W, 14.7°S)
Winia Fluctus (30°W, 45°N)	Rohe Fluctus (37.8°W, 47.3°N)	Mohini Fluctus (38.5°W, 11.8°S)
	Tui Regio (125°W, 24°S)	Erebor Mons (36.2°W, 5.0°S)
		Hotei Regio (78°W, 26°S)

ammonia usually considered in experimental simulation works was 10–25 wt % (Neish *et al.*, 2009; Poch *et al.*, 2012). However, a recent study shows that the fraction of ammonia in the subsurface ocean could be lower, around 2–3 wt % if taking into account the actual mass of nitrogen in Titan's atmosphere (Tobie *et al.*, 2012). Additionally, studies have provided new highlights on the bulk composition of Titan for various gas species. Indeed, Saturn's observed atmosphere enrichment constrains the composition of the planetesimals present in the feeding zone of Saturn. The enrichment in volatiles in Saturn's atmosphere has been reproduced by assuming (Hersant *et al.*, 2004, 2008) that (i) carbon is mostly in the form of CH_4 clathrate hydrates and condensed CO_2; (ii) nitrogen is mostly in the form of NH_3 hydrates; (iii) sulfur is mostly in the form of H_2S clathrate hydrates. In the present study, we assumed that those gas species have been trapped in the likely internal ocean. By taking into account the plausible acid-base properties of a water-ammonia ocean, a new probable composition of the cryomagma that could potentially interact with Titan's deposited aerosols has been determined (see Section 2.2).

In this work, hydrolyses were performed on Titan aerosol analogues with 5 wt % ammonia aqueous solution with and without salts (Na_2CO_3 and NaHS) in order to simulate the new probable composition of the cryomagma described above. Previous experiments have tested different kinds of hydrolyses: (i) acidic pH hydrolysis with HCl 6 mol L^{-1} (Khare *et al.*, 1986; Nguyen, 2007; Taniuchi *et al.*, 2013), HCl 2 mol L^{-1} (Nguyen, 2007); (ii) hydrolysis at pH 7 (Nguyen, 2007); (iii) basic pH hydrolysis with 25 wt % NH_3 (Ramirez *et al.*, 2010; Poch *et al.*, 2012), with 13 wt % NH_3 (Neish *et al.*, 2009; Ramirez *et al.*, 2010) or less (Ramirez *et al.*, 2010). The experimental conditions of these works are summarized below in Section 3.2. Amino acids, alcohols, carboxylic acids, urea, and nucleobases have been identified as hydrolysis products. Only two studies have reported quantitative data on the production of these organics of astrobiological interest (Ramirez *et al.*, 2010; Poch *et al.*, 2012).

The experimental device used to synthesize representative free-oxygen analogues of Titan's aerosols (named Titan tholins) is detailed, as well as the calculation of the molar concentration of each minor species that could constitute the likely subsurface ocean. The detection/identification/quantification methods of hydrolysis products are described and the results related to the low-temperature alkaline pH hydrolysis of oxygen-free Titan tholins are presented and discussed.

2. Experimental

2.1. Plasma experimental setup

To synthesize representative analogues of Titan aerosols, the experimental setup (developed at LISA, Créteil, France) named PLASMA has been used (Coll *et al.*, 1997). This device allows for simulation of the dissociation of the main gas molecules present in Titan's atmosphere by the establishment of a cold plasma in a gas mixture of N_2 and CH_4.

As shown in Fig. 1, the reactor is connected to a gas cylinder composed of a mixture of N_2/CH_4 (98/2 ratio), which

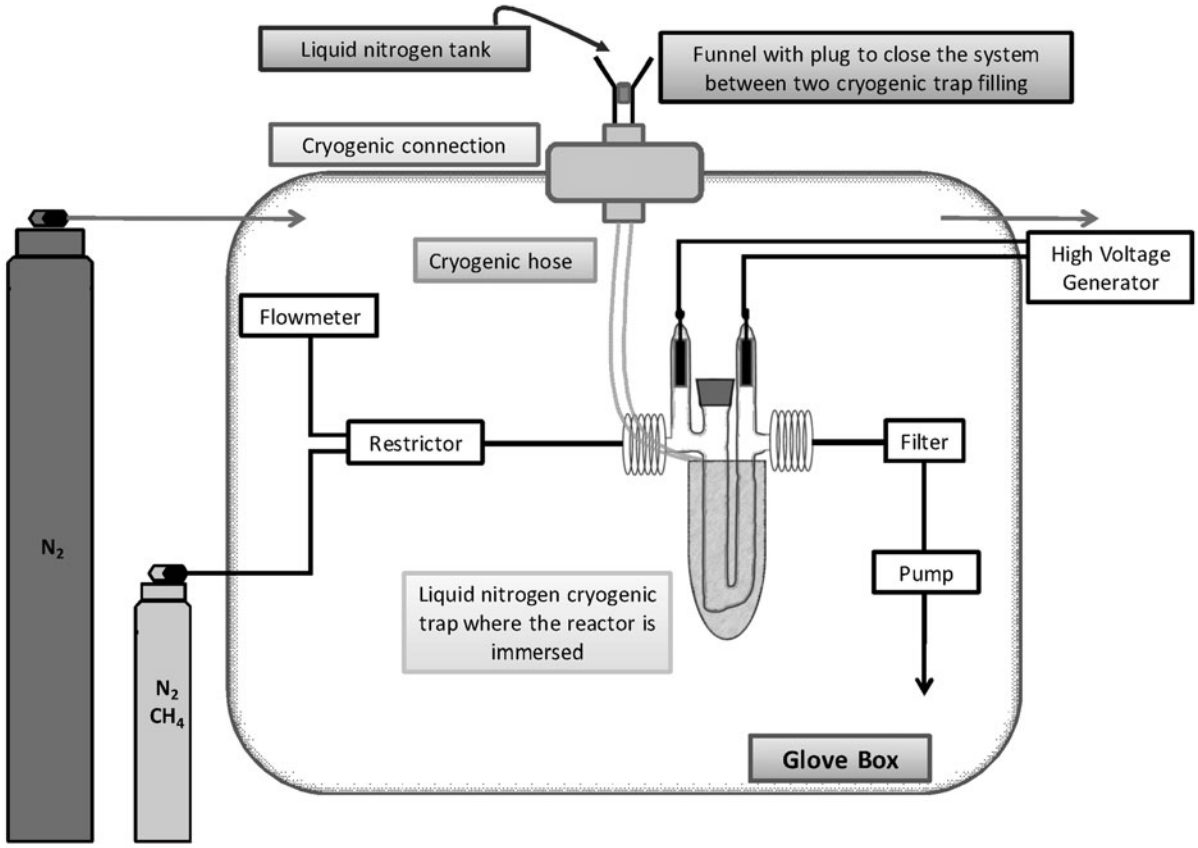

FIG. 1. Scheme of the experimental setup, named PLASMA, used for the synthesis of Titan tholins.

is representative of the mean gas composition of Titan's atmosphere. This gas mixture continuously flows through the reactor, which allows for maintenance of the N_2/CH_4 ratio constant during the synthesis. A flowmeter/restrictor (Bronkhorst F-201CV-100-AAD-11-V) placed at the cylinder exit and upstream of the reactor maintains a constant gas flow of 20 sccm (1 sccm = 7.4×10^{-7} mol s^{-1}: standard cubic centimeters per minute) and a pressure of 2.6 mbar. A dry pump (Edwards nXDS6i, maximum pumping speed = 6.2 m^3 h^{-1}) is used to maintain the low pressure in the system.

By using a high-voltage generator, an electric discharge (2 kV–23.2 mA) is applied on the gas mixture, which establishes a cold plasma that induces the dissociation of N_2 and CH_4 and other chemical reactions leading to the formation of tholins that settle on the reactor's wall. The U-shape of the reactor (Fig. 1) facilitates the introduction of the tholins into a Dewar vessel full of liquid nitrogen and allows the simulation to continue at a very low temperature. However, in the present study, the synthesis was conducted only at ambient temperature since the production yields of tholins, at low temperature, are too low to provide the quantity of tholins necessary to achieve this new and exploratory experimental study.

Previous studies have shown that tholins synthesized with the PLASMA experimental setup were contaminated by the atmospheric molecular oxygen of the laboratory (Poch *et al.*, 2012). Consequently, the entire experimental device, with the exception of the N_2/CH_4 gas cylinder and the high-voltage generator, were put into a glove box to insulate the experiment from the terrestrial atmosphere. The glove box was connected to a N_2 gas cylinder to maintain a high pressure of internal gas in it. Moreover, silica gel granules were placed in the glove box to capture the residual water vapor. After 3 days and nights of synthesis, the condensed tholins are collected by scratching the reactor's walls. This step occurred in the glove box as well.

2.2. Plausible subsurface ocean chemical composition: theoretical calculation

The chemical composition of the cryomagma is likely in close association with the chemical composition of the potential subsurface ocean. So to simulate the cryovolcanism area (assumed to be made of cryomagma), we determined the possible chemical composition of the internal ocean. Models of the formation of Titan suggest that the water ocean was initially in contact with the atmosphere (Fortes, 2000). We assumed that the composition of the present ocean is similar to that of the early ocean, and neglected the pressure effect on the pH and the solubility.

If we consider that this ocean is only composed of 5 wt % NH_3, that is, 2.88 mol L^{-1}, then its pH can be determined with the classical weak base formula:

$$\mathrm{pH} = 7 + \frac{1}{2}(\mathrm{pKa} + \log(\mathrm{NH_3}))$$

With pKa = 9.2, it comes to pH = 11.83, corresponding to $(H^+) = 1.5\times10^{-12}$ mol L^{-1}.

Knowledge of the molar concentration of ammonia and the plausible acid-base properties of the water-ammonia ocean allow for calculation of the concentration of the other minor species, which include NH_4^+, OH^-, H_2S, HS^-, S^{2-}, $CO_2(aq)$, HCO_3^-, CO_3^{2-}.

2.2.1. NH_4^+/NH_3.

We assume a concentration of 5 wt % of ammonia. This is equivalent to the molar concentration:

$$\mathbf{(NH_3) = 5\ wt\ \% = 2.88\ mol\ L^{-1}}$$

Then with the acid dissociation constant Ka

$$\mathrm{Ka} = \frac{(\mathrm{NH_3})\cdot(\mathrm{H^+})}{(\mathrm{NH_4^+})}$$

With a pKa of 9.2 and a pH of 11.83, it comes to

$$\mathbf{(NH_4^+) = 6.8\times10^{-3}\ mol\ L^{-1}}$$

2.2.2. H^+/OH^-.

The concentration of H^+ is directly deduced from the pH value

$$\mathbf{(H^+) = 1.5\times10^{-12}\ mol\ L^{-1}}$$

And following in the same way, from the water equilibrium, the concentration of OH^- is obtained by using the expression

$$(\mathrm{OH^-}) = 10^{-(14-\mathrm{pH})}$$

Then the value of the hydroxide concentration is

$$\mathbf{(OH^-) = 6.8\times10^{-3}\ mol\ L^{-1}}$$

2.2.3. $H_2S/HS^-/S^{2-}$.

For carbon dioxide and hydrogen sulfide, another parameter was needed to determine their maximum concentration: their solubility in water for the likely ocean's temperature.

At the temperature of $T = 262$ K, the solubility of H_2S is 8.7 $g_{(H_2S)}/kg_{(H_2O)}$. So the maximum concentration for sulfurs in water is

$$C_{\max} = C_0 = 0.256\ \mathrm{mol\ L^{-1}}$$

The mass balance for sulfides gives the following expression:

$$C_0 = (\mathrm{H_2S}) + (\mathrm{HS^-}) + (\mathrm{S^{2-}})$$

We can also write

$$C_0 = (\mathrm{S^{2-}})\left(1 + \frac{(\mathrm{HS^-})}{(\mathrm{S^{2-}})} + \frac{(\mathrm{H_2S})}{(\mathrm{S^{2-}})}\right)$$

With

$$\mathrm{Ka_1} = \frac{(\mathrm{HS^-})\cdot(\mathrm{H^+})}{(\mathrm{H_2S})} \quad \text{and} \quad \mathrm{Ka_2} = \frac{(\mathrm{S^{2-}})\cdot(\mathrm{H^+})}{(\mathrm{HS^-})}$$

it comes to

$$C_0 = (S^{2-})\left(1 + \frac{(H^+)}{Ka_1} + \frac{(H^+)^2}{Ka_1 Ka_2}\right)$$

$$(H_2S) = (HS^-)\cdot\left(\frac{(H^+)}{Ka_1}\right) \text{ and } (S^{2-}) = (HS^-)\cdot\left(\frac{Ka_2}{(H^+)}\right)$$

Then

$$(HS^-) = \frac{C_0}{\left(\frac{(H^+)}{Ka_1}\right) + 1 + \left(\frac{Ka_2}{(H^+)}\right)}$$

With $Ka_1 = 10^{-7}$ and $Ka_2 = 10^{-12.9}$ at pH = 11.83, we get

$$\mathbf{(HS^-) = 0.236\ mol\ L^{-1}}$$

$$(S^{2-}) = (HS^-)\cdot\left(\frac{Ka_2}{(H^+)}\right)$$

$$\mathbf{(S^{2-}) = 0.020\ mol\ L^{-1}}$$

and

$$(H_2S) = (HS^-)\cdot\left(\frac{(H^+)}{Ka_1}\right)$$

$$\mathbf{(H_2S) = 3.491\times10^{-6}\ mol\ L^{-1}}$$

2.2.4. $CO_2(aq)/HCO_3^-/CO_3^{2-}$. As for sulfides, we need the solubility of carbonates in water to determine the concentration of all their species.

For a temperature of $T = 262$ K, the solubility of CO_2 is 4.2 $g_{(CO_2)}/kg_{(H_2O)}$. So the maximum concentration of carbonates in water is

$$C'_{max} = C'_0 = 0.095\ \text{mol L}^{-1}$$

With

$$C'_0 = (CO_2) + (HCO_3^-) + (CO_3^{2-})$$

this expression becomes

$$C'_0 = (CO_2)\left(1 + \frac{(HCO_3^-)}{(CO_2)} + \frac{(CO_3^{2-})}{(CO_2)}\right)$$

With

$$K'a_1 = \frac{(HCO_3^-)\cdot(H^+)}{(CO_2)} \quad \text{and} \quad K'a_2 = \frac{(CO_3^{2-})\cdot(H^+)}{(HCO_3^-)}$$

then it becomes

$$C'_0 = (CO_3^{2-})\left(1 + \frac{(H^+)}{K'a_2} + \frac{(H^+)^2}{K'a_2 K'a_1}\right)$$

$$(CO_2) = (HCO_3^-)\cdot\left(\frac{(H^+)}{K'a_1}\right) \text{ and}$$

$$(CO_3^{2-}) = (HCO_3^-)\cdot\left(\frac{K'a_2}{(H^+)}\right)$$

Then

$$(HCO_3^-) = \frac{C'_0}{\left(\frac{(H^+)}{K'a_1}\right) + 1 + \left(\frac{K'a_2}{(H^+)}\right)}$$

With $K'a_1 = 10^{-6.4}$ and $K'a_2 = 10^{-10.3}$ at pH = 11.83, we get

$$\mathbf{(HCO_3^-) = 2.72\times10^{-3}\ mol\ L^{-1}}$$

$$(CO_3^{2-}) = (HCO_3^-)\cdot\left(\frac{K'a_2}{(H^+)}\right)$$

$$\mathbf{(CO_3^{2-}) = 0.092\ mol\ L^{-1}}$$

and

$$(CO_2) = (HCO_3^-)\cdot\left(\frac{(H^+)}{K'a_1}\right)$$

$$\mathbf{(CO_2) = 3.6\times10^{-6}\ mol\ L^{-1}}$$

2.2.5. Na^+. Since the presence of sodium salt (as sodium carbonate for example) in the ocean is now suspected (Mitri *et al.*, 2014), we have chosen to use the Na^+ ion as a counter ion to get the electroneutrality in the ocean. By applying the electroneutrality law to the mixture, we get the following expression:

$$(HCO_3^-) + 2(CO_3^{2-}) + (HS^-) + 2(S^{2-}) + (OH^-) = (H^+) + (Na^+) + (NH_4^+)$$

Then, it comes to

$$\mathbf{(Na^+) = 0.463\ mol\ L^{-1}}$$

Table 2 summarizes the possible chemical composition of the likely subsurface ocean. Hydrogenosulfide and carbonate anions appear to be among the most abundant minor species.

TABLE 2. POSSIBLE CHEMICAL COMPOSITION OF THE LIKELY SUBSURFACE OCEAN FOR A PH OF 11.83

Species	NH_3	NH_4^+	H^+	HO^-	$CO_2(aq)$	HCO_3^-	CO_3^{2-}	H_2S	HS^-	S^{2-}	Na^+
C (mol/L)	**2.88**	6.8×10^{-3}	1.5×10^{-12}	6.8×10^{-3}	3.6×10^{-6}	2.7×10^{-3}	**0.092**	3.5×10^{-6}	**0.236**	0.020	0.463

Table 3. Values of the Activity Coefficients, Activities, and pH When Ocean Temperature and Salts Are Taken into Account

T (K)	262	270	298
A ($M^{-1/2}$)	0.61	0.58	0.50
Υ1	0.71	0.73	0.76
Υ2	0.26	0.28	0.33
pH	11.76	11.76	11.77

2.2.6. The influence of the ocean's temperature on the pH value. The previous calculated pH value is valid at an ambient temperature of 298 K. However, Titan's ocean temperature would be close to 262 K (lower limit of the ocean)/270 K (upper limit of the ocean) (Tobie *et al.*, 2012).

To determine the influence of the ocean's temperature and the ionic strength on the pH value, the Davies approach (Butler, 1998) has been followed to estimate the ion activity coefficients for each temperature.

$$\gamma_i = 10^{-\left(A z_i^2 \cdot \left(\frac{\sqrt{I}}{1+\sqrt{I}} - 0.3I\right)\right)}$$

With

γ_i = ion activity coefficient
I = ionic strength
z_i = charge of the ion i
A = parameter depending on the temperature (T) and the dielectric constant (ε)
$= 1.82 \times 10^6 \times (\varepsilon T)^{-3/2}$

Since liquid water is the solvent, we use the dielectric constant of water for the calculations, ignoring the presence of ammonia. Its value is given by the *Handbook of Chemistry and Physics*, 87th edition (Lide, 2006, p 6–133).

$$\varepsilon_{(H_2O)} = 80.1$$

The ionic strength I is given by the following equation:

$$I = \frac{1}{2}\sum_i C_i z_i^2$$

With this new calculation method, it is possible to avoid the initial assumption, which was that the ion activity coefficient $\gamma_i = 1$.

By using the calculated concentration from Table 2, it is possible to determine the potential ionic strength of the internal ocean.

$$I = \frac{1}{2}\left((HCO_3^-) + 4(CO_3^{2-}) + (HS^-) + 4(S^{2-}) + (OH^-) + (H^+) + (Na^+) + (NH_4^+)\right)$$

$$I = 0.757 \text{ mol L}^{-1}$$

It is now possible to obtain the average ion activity coefficient at different temperatures.

For $z_i = \pm 1$, we get γ_1

$$\gamma_1 = \gamma_{(H^+)} = \gamma_{(Na^+)} = \gamma_{(HCO_3^-)} = \gamma_{(HS^-)} = \gamma_{(OH^-)} = \gamma_{(NH_4^+)}$$

which can be obtained with the Davies approach as mentioned previously

$$\gamma_1 = 10^{-\left(A \cdot \left(\frac{\sqrt{I}}{1+\sqrt{I}} - 0.3I\right)\right)}$$

For $z_i = \pm 2$, we get γ_2

$$\gamma_2 = \gamma_{(CO_3^{2-})} = \gamma_{(S^{2-})}$$

and

$$\gamma_2 = 10^{-\left(4A \cdot \left(\frac{\sqrt{I}}{1+\sqrt{I}} - 0.3I\right)\right)}$$

Finally, it is possible to calculate accurately the pH value by taking into account the ocean temperature.

$$pH = 7 + \frac{1}{2}\left(pKa + \log\left(\gamma_1^T \cdot [NH_3]\right)\right)$$

Table 3 displays the results concerning the ion activity coefficients and the corrected pH values. We can see that the pH in the ocean would more likely be 11.76. So it seems that the temperature and the presence of salts in the ocean do not impact strongly the pH value.

Indeed, the molar concentration of the minor species has been recalculated for a pH of 11.76 as shown in Table 4. Then, we show that the values obtained are not significantly different from those calculated at pH 11.83, especially for the most abundant minor species HS^- and CO_3^{2-}.

Those new data have been included in our hydrolysis experiments as detailed in the following section.

2.3. Hydrolysis conditions

To integrate this new plausible composition of the cryomagma in our hydrolysis experiments, four different kinds of hydrolysis were performed on 10 mg of oxygen-free tholins as indicated in Table 5.

All hydrolysis solutions included 5 wt % of ammonia in water. One has carbonate also (hydrolysis n°3); another one has sulfide (hydrolysis n°2). The last one (hydrolysis n°4) has both carbonate and sulfide in order to identify the contribution of each species in the production of organics. Each hydrolysis was studied at three different temperatures: 293,

Table 4. Possible Chemical Composition of the Likely Subsurface Ocean for a pH of 11.76

Species	NH_3	NH_4^+	H^+	HO^-	CO_2(aq)	HCO_3^-	CO_3^{2-}	H_2S	HS^-	S^{2-}	Na^+
C (mol/L)	**2.88**	7.9×10^{-3}	1.7×10^{-12}	5.8×10^{-3}	1.4×10^{-8}	3.2×10^{-3}	**0.092**	4.2×10^{-6}	**0.239**	0.017	0.458

TABLE 5. EXPERIMENTAL CONDITIONS FOR THE DIFFERENT ALKALINE pH HYDROLYSES

	Hydrolysis n°1	Hydrolysis n°2	Hydrolysis n°3	Hydrolysis n°4
NH_3	5 wt%	5 wt%	5 wt%	5 wt%
CO_3^{2-} (mol.L^{-1})	-	-	0.092	0.092
HS^- (mol.L^{-1})	-	0.236	-	0.236
Temperature	293 K, 279 K, 253 K			
Evolution time	10 weeks			

279, and 253 K. For each kind of hydrolysis, reference solutions were placed in the same experimental conditions.

2.4. Gas chromatography–mass spectrometry

After 10 weeks of evolution at the three different temperatures mentioned above, the aqueous phase was analyzed by gas chromatography–mass spectrometry using a Thermo Scientific TRACE gas chromatograph (GC) coupled to a Thermo Scientific PolarisQ mass spectrometer (MS; trap ion detection mode). The PTV injector was heated at 250°C with a split ratio of 1/25. The GC column was a fused silica capillary Phenomenex Zebron Inferno ZB-5HT (L = 30 m × i.d. = 0.25 mm × dt = 0.25 μm). Its almost apolar stationary phase (5% phenyl and 95% dimethylpolysiloxane) was efficient to separate derivatized products, which are molecules of very low polarity. The GC temperature program started at 70°C for 5 min, then with a temperature gradient of 6°C/min it increased from 70°C to 350°C, and finally it stayed 5 min more at 350°C. The carrier gas used was helium (99.9999%) with a constant flow of 1 mL min^{-1}. To protect the filament from derivatization reagents, the start time of scan began after the first 8 min, allowing the remaining derivatization agents to be fully eluted. The electronic impact source was set at 70 eV, and the mass ranged from 40 to 550 *m/z*.

2.5. Characterization of hydrolysis products: derivatization and extraction phase

The GCMS analytical device requires a derivatization step for decreasing the polarity and increasing the stability and volatility of most of the produced organics, allowing for the analysis of compounds of astrobiological interest. Indeed, amino acids, carboxylic acids, and nucleobases are very polar and of low volatility. As described in Fig. 2, *N*-methyl-*N*-(*tert*-butyldimethylsilyl)-trifluoroacetamide (MTBSTFA) with dimethylformamide (DMF) as a solvent has been used as a derivatization solution (Buch *et al.*, 2006, 2009). A total of 30 μL of MTBSTFA and 10 μL of DMF were added to each sample (and to each reference solution), which had been dried before, under a nitrogen flow at 40°C. This mixture was heated at 75°C for 15 min to perform the derivatization reaction.

Before each sample injection, two blank analyses were performed. The first one was a real blank without any injection, and the second one was an injection with only the derivatization reagent. In this way, we were able to identify the GC peaks directly produced by the derivatization reagent and solvent.

To characterize the products, their respective standards were analyzed, and a database of derivatized molecules was established, as detailed in Table 6.

2.6. Influence of salt on the derivatization reaction

In the presence of salts, which includes all samples except for hydrolysis n°1, an additional step is needed before the derivatization in order to eliminate the salts, which could interfere with the derivatization. For that purpose, the sample was eluted from a cationic exchange resin. This step was performed with an AG 50W-X8 resin #142-1441 (Biorad Laboratories, Inc.) so that neutral molecules and anions do not interact with the resin. Once the sample was dried up, pure distilled water was added in order to eliminate the ammonia (to avoid converting the counter-ions in the resin from H^+ to NH_4^+). Indeed, the counter-ions in the resin (here H^+) are substituted by ions present in the sample that have the same charge (here Na^+). In that case, by removing

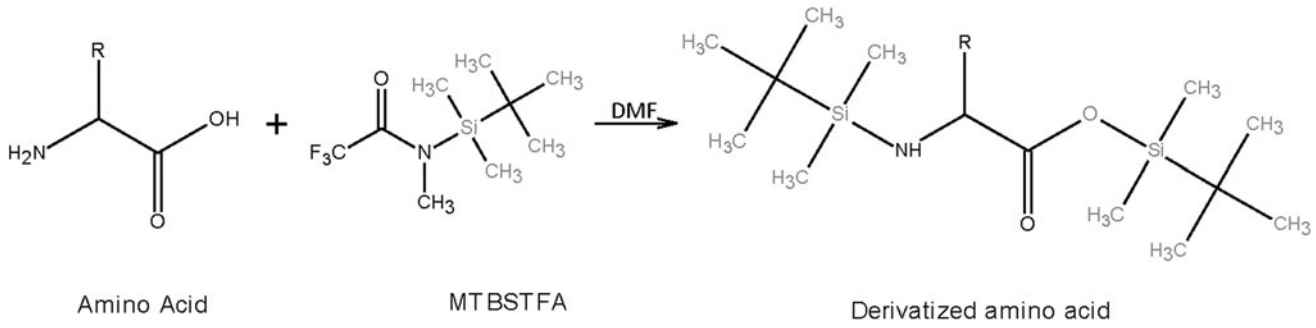

FIG. 2. Scheme of the MTBSTFA derivatization reaction.

Table 6. Database of Derivatized Molecules of Astrobiological Interest

	Molecules	CAS	Formula	Retention time (min)	Mass fragments (bold) and their relative intensity (‰)
Internal standard	Methyl laurate	111-82-0	$C_{13}H_{26}O_2$	20.79-20.82	**74** 999 | **87** 557 | **41** 245 | **43** 204 | **55** 191 | **29** 120 | **75** 119 | **57** 98 | **69** 98 | **143** 77 |
Proteic amino acids	Alanine 2-tbdms	92751-15-0	$C_{15}H_{35}NO_2Si_2$	21.00-21.06	**73** 999 | **158** 743 | **147** 499 | **232** 404 | **260** 267 | **59** 210 | **57** 196 | **41** 168 | **75** 152 | **45** 132 |
	Glycine 2-tbdms	107715-88-8	$C_{14}H_{33}NO_2Si_2$	21.45-21.49	**73** 999 | **147** 764 | **218** 480 | **246** 273 | **59** 202 | **57** 189 | **41** 177 | **75** 160 | **45** 137 | **148** 131 |
	Aspartic acid 3-tbdms	107715-96-8	$C_{22}H_{49}NO_4Si_3$	31.74-31.74	**73** 999 | **292** 334 | **218** 325 | **147** 300 | **61** 208 | **75** 201 | **59** 193 | **320** 188 | **57** 157 | **41** 150 |
	Urea 2-tbdms	82475-73-8	$C_{13}H_{32}N_2OSi_2$	23.22-23.25	**231** 999 | **147** 854 | **73** 513 | **232** 201 | **74** 158 | **132** 146 | **41** 146 | **148** 136 | **57** 130 | **75** 113 |
No proteic amino acids	α-aminobutyric acid 2-tbdms	82112-33-2	$C_{16}H_{37}NO_2Si_2$	22.12-22.13	73 999 | 172 764 | 246 427 | 147 359 | 274 269 | 59 220 | 57 196 | 41 176 | 75 152 | 45 120 |
	N-Acetylglycine 2-tbdms	NIST# 221667	$C_{16}H_{35}NO_3Si_2$	25.23	**73** 999 | **75** 282 | **116** 278 | **288** 272 | **147** 233 | **57** 136 | **59** 133 | **41** 126 | **55** 120 | **45** 111 |
	Beta alanine 2-tbdms	110024-88-9	$C_{15}H_{35}NO_2Si_2$	23.02-23.04	**73** 999 | **218** 700 | **147** 544 | **144** 532 | **260** 259 | **59** 253 | **75** 238 | **57** 233 | **41** 226 | **80** 189 |
	Sarcosine 2-tbdms	110024-89-0	$C_{15}H_{35}NO_2Si_2$	22.18-22.20	**73** 999 | **147** 464 | **158** 342 | **232** 316 | **59** 224 | **57** 191 | **260** 187 | **41** 165 | **45** 139 | **75** 120 |
	γ-aminobutyric acid 2-tbdms	110024-92-5	$C_{16}H_{35}NO_3Si_2$	25.19-25.21	**73** 999 | **147** 976 | **75** 582 | **274** 448 | **59** 259 | **41** 225 | **142** 181 | **57** 170 | **148** 162 | **74** 137 |
	Homoserine 3-tbdms	NIST# 221666	$C_{22}H_{51}NO_3Si_3$	30.77-30.79	**73** 999 | **302** 232 | **404** 196 | **89** 179 | **376** 175 | **57** 145 | **59** 121 | **147** 117 | **75** 115 | **41** 111 |
Carboxylic acids - Alcohols	Succinic acid 2-tbdms	98847-52-0	$C_{16}H_{34}O_4Si_2$	25.22-25.23	**73** 999 | **75** 417 | **147** 405 | **289** 289 | **41** 142 | **57** 126 | **55** 115 | **45** 107 | **74** 102 | **59** 92 |
	Palmitic acid 2-tbdms	58160-87-5	$C_{22}H_{46}O_2Si$	33.51-33.52	**313** 999 | **75** 489 | **314** 290 | **129** 178 | **43** 151 | **73** 130 | **41** 110 | **117** 92 | **131** 92 | **315** 75 |
	Stearic acid 2-tbdms	87020-51-7	$C_{24}H_{50}O_2Si$	36.25-36.27	**341** 999 | **75** 651 | **43** 323 | **342** 274 | **41** 213 | **129** 200 | **73** 188 | **57** 145 | **55** 118 | **131** 112 |
	Crotonic acid 1-tbdms	86254-80-0	$C_{10}H_{20}O_2Si$		**143** 999 | **75** 763 | **41** 322 | **99** 286 | **69** 228 | **39** 192 | **45** 141 | **47** 124 | **144** 117 | **73** 106 |
	Glycerol 3-tbdms	82112-23-0	$C_{21}H_{50}O_3Si_3$	27.32-27.34	**89** 999 | **73** 914 | **147** 476 | **171** 272 | **189** 266 | **133** 228 | **115** 190 | **377** 141 | **41** 103 | **59** 99 |
	Oxalic acid 2-tbdms	104255-91-6	$C_{14}H_{30}O_4Si_2$	21.23-21.25	**73** 999 | **147** 636 | **75** 323 | **59** 298 | **45** 275 | **115** 249 | **41** 179 | **133** 169 | **58** 159 | **57** 149 |
	Methylsuccinic acid 2-tbdms	98830-33-2	$C_{17}H_{36}O_4Si_2$	25.39-25.40	**73** 999 | **147** 456 | **75** 444 | **303** 261 | **41** 213 | **57** 149 | **45** 106 | **74** 104 | **59** 99 | **69** 78 |

Na^+ (replaced by H^+) in the sample solution, Na_2CO_3 does not form, so the derivatization can occur as usual.

The sample was introduced into the hydrated resin with a Pasteur pipette and collected at the exit: this was solute n°1. Next, to recover carboxylic acids and amino acids trapped by the resin, a solution of ammonia was added to the resin: solute n°2 was collected. Finally, for recovering poor water soluble carboxylic acids, an aqueous solution of ethanol was introduced into the resin: solute n°3 was collected. Those three solutes were then dried separately before being derivatized (as detailed above in this section). This step was efficient for hydrolysis containing only carbonates (*i.e.*, hydrolysis n°3). However, we have been unable, to date, to perform this extraction step correctly on samples that contain sulfur (*i.e.*, hydrolysis n°2 and n°4). To resolve this issue, we plan to use a UHPLC analytical technique.

Table 7. Review of the Calibration Curve of Several Organics Detected after Hydrolysis

	Injected quantity after split ratio (pmol)	Linear regression equation	R^2
Alanine	11.4-114	y = 1E+10x - 0.0091	0.9738
Glycine	11.4-114	y = 1E+10x - 0.0693	0.9925
Aspartic acid	11.4-114	y = 2E+10x - 0.1244	0.9842
Oxalic acid	14.5-145	y = 7E+9x - 0.0464	0.9969
Succinic acid	11.4-114	y = 3E+9x - 0.0219	0.9963
Methylsuccinic acid	11.4-114	y = 3E+9x - 0.0278	0.9912
α-aminobutyric acid	11.2-112	y = 2E+10x - 0.0571	0.979
Urea	24.1-241	y = 4E+9x - 0.007	0.9698
Beta Alanine	11.6-116	y = 1E+10x - 0.056	0.9791
N-Acetylglycine	10.8-108	y = 3E+8x - 0.0006	0.9474
Palmitic acid	10.5-105	y = 9E+9x - 0.1544	0.977
Stearic acid	11.4-114	y = 9E+9x - 0.1627	0.9805
Sarcosine	13.6-136	y = 2E+9x - 0.0346	0.9415
γ-aminobutyric acid	13.6-136	y = 2E+9x - 0.0162	0.9837
Glycerol	11.4-114	y = 2E+9x - 0.0192	0.9787
Homoserine	11.4-114	y = 6E+8x - 0.0047	0.9502

2.7. Hydrolysis products' quantification and production yields

To quantify and determine the production yields of the compounds produced from the hydrolysis step, 4 μL of an internal standard, methyl-laurate at 7.9×10^{-2} mol L^{-1} (Fluka, 97%), was added to each derivatized solution before the injection in the GCMS. To achieve quantitative measurements, we carried out a calibration curve for each targeted compound. For each molecule, a calibration curve (see Table 7) was traced by using the ratio of the chromatographic peak area of the compound over the chromatographic peak area of the internal standard (methyl-laurate) as a function of the amount of the targeted compound. Then by using the calibration curve (Table 7) it was possible to determine the exact quantification of the molecules produced after hydrolysis. The production yields were obtained by calculating the ratio of the mass of the product to the mass of hydrolyzed tholins.

To obtain a faithful quantification, for each injection made for the calibration and for the sample, a minimum of three replicas was achieved. Those replicas allowed us to formulate accurate error bars for each value.

3. Results

The chromatogram acquired for nonhydrolyzed tholins after derivatization (as detailed in Section 2.5) is shown in Fig. 3. It can be seen that the chromatogram does not display any oxygenated molecules. This demonstrates that the identified products from the hydrolysis experiments are due to the hydrolysis of tholins and not to oxygen contamination (from the air) of the tholins and guarantees the reliability of the data presented in this paper.

3.1. Hydrolysis with and without carbonates

Figure 4 shows an example of a chromatogram obtained by gas chromatography–mass spectrometry analysis of tholin hydrolysis. The chromatogram displayed is related to the hydrolysis of free-oxygen tholins in a water-ammonia mixture at 293 K after derivatization and reports the hydrolysis products identified. Moreover, Fig. 5 presents the whole set of data obtained for the two different experiments: hydrolysis n°1 and hydrolysis n°3. As presented in Table 5, hydrolysis n°1 resulted from the water-ammonia (5 wt %) mixture alone, whereas hydrolysis n°3 includes carbonates. Figure 5 provides the production yields for each hydrolysis product displayed as histograms. The production yields have been multiplied by 10^6 to fit with this figure. The color code refers to the evolution temperature: the highest temperature is in black (293 K), the middle one in gray (279 K), and the lowest in white (253 K).

For hydrolysis n°3, only data for two temperatures are reported. The data obtained for the lowest evolution temperature are not reported because they are not reliable due to technical issues during the gas chromatography–mass spectrometry analysis.

Table 8 sums up the production yield values of each hydrolysis product displayed in Fig. 5 but without multiplication factor in order to facilitate the reading of Fig. 5.

Several astrobiologically interesting organics were characterized after free-oxygen tholin hydrolysis. The production of amino acids, carboxylic acids, and fatty acids is observed for both hydrolyses. For hydrolysis n°1, 12 products were identified: alanine, glycine, urea, α-aminobutyric acid, γ-aminobutyric acid, *N*-acetylglycine, β-alanine, oxalic acid, succinic acid, methylsuccinic acid, palmitic acid, and

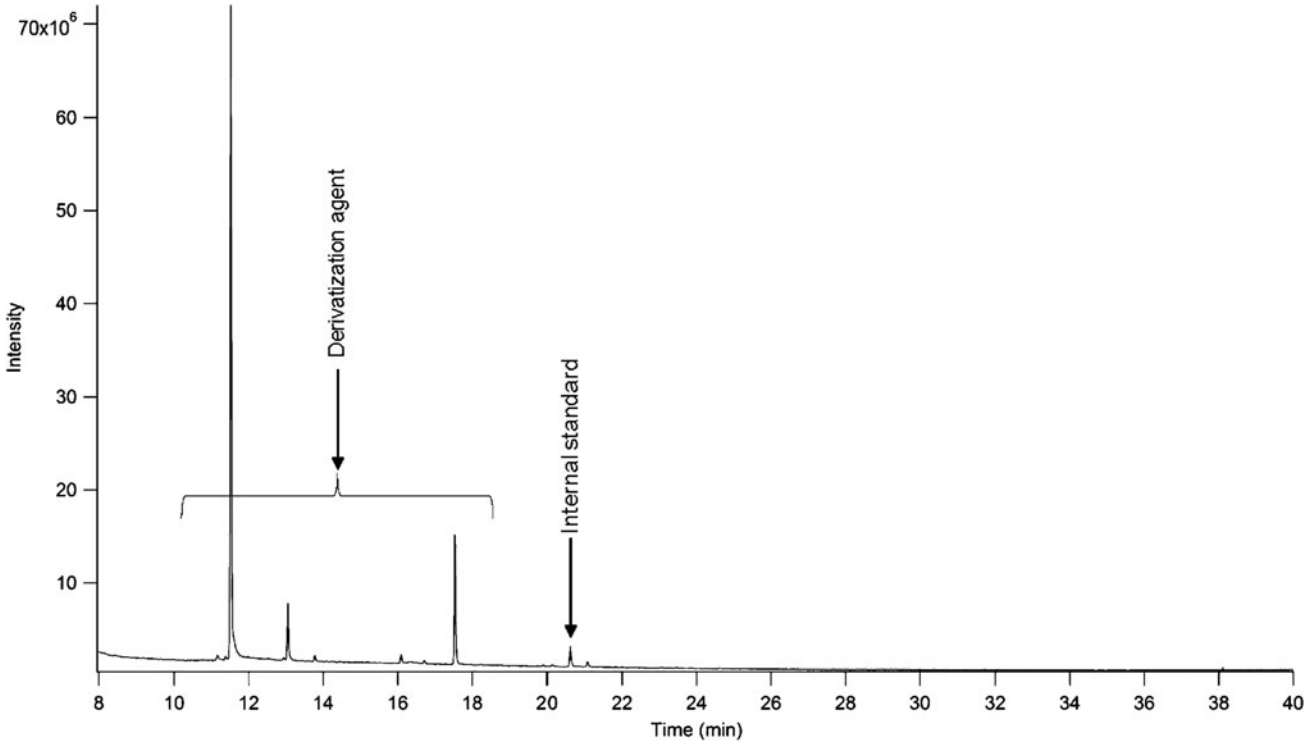

FIG. 3. Chromatogram of a derivatized sample of nonhydrolyzed tholins. Positions of the chromatographic peaks of compounds identified by their standards are shown by arrows. The 30 m × 0.25 mm × 0.25 μm Zebron Inferno ZB-5HT column, operated in the split mode (1:25), was programmed at 6°C min^{-1} from 70°C to 300°C with an inlet flow of helium of 1 mL min^{-1}.

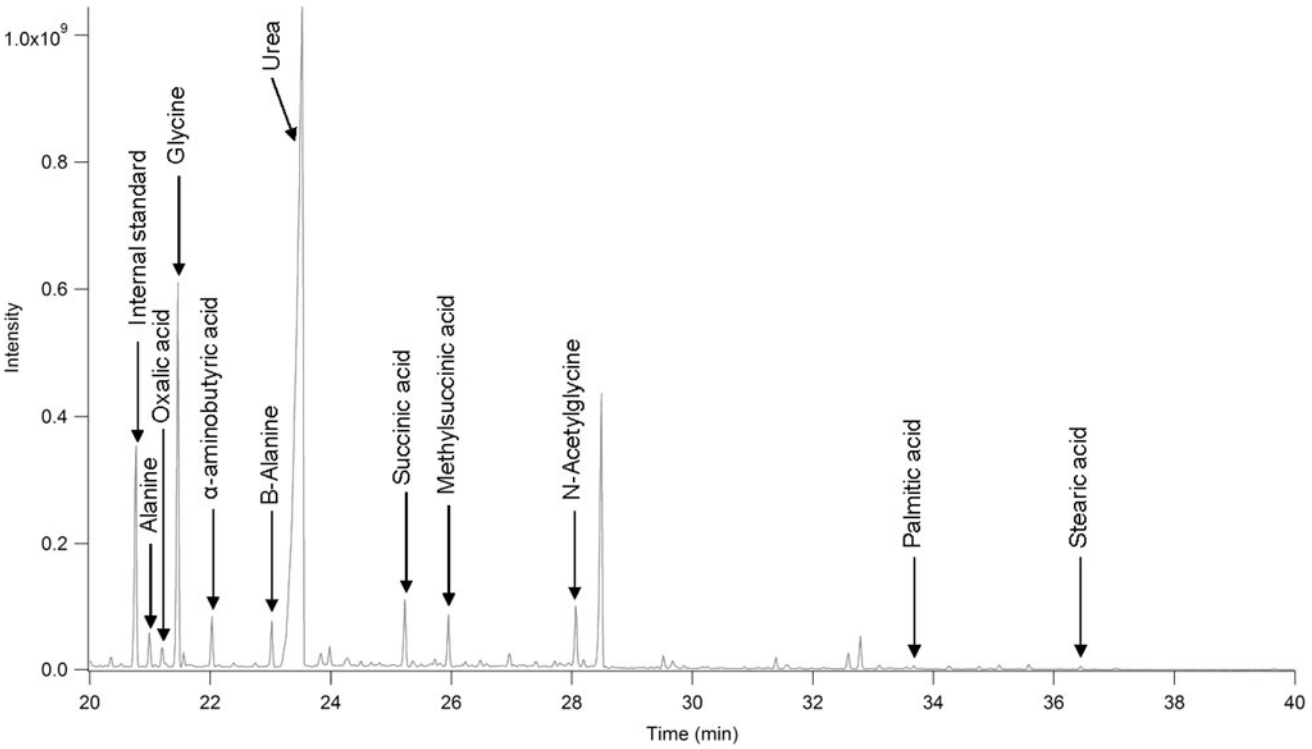

FIG. 4. Chromatogram of a derivatized sample of hydrolyzed tholins in water-ammonia (5 wt % NH_3—hydrolysis n°1) mixture at 293 K after derivatization. Positions of the chromatographic peaks of compounds identified by their standards are shown by arrows. The 30 m × 0.25 mm × 0.25 μm Zebron Inferno ZB-5HT column, operated in the split mode (1:25), was programmed at 6°C min^{-1} from 70°C to 300°C with an inlet flow of helium of 1 mL min^{-1}.

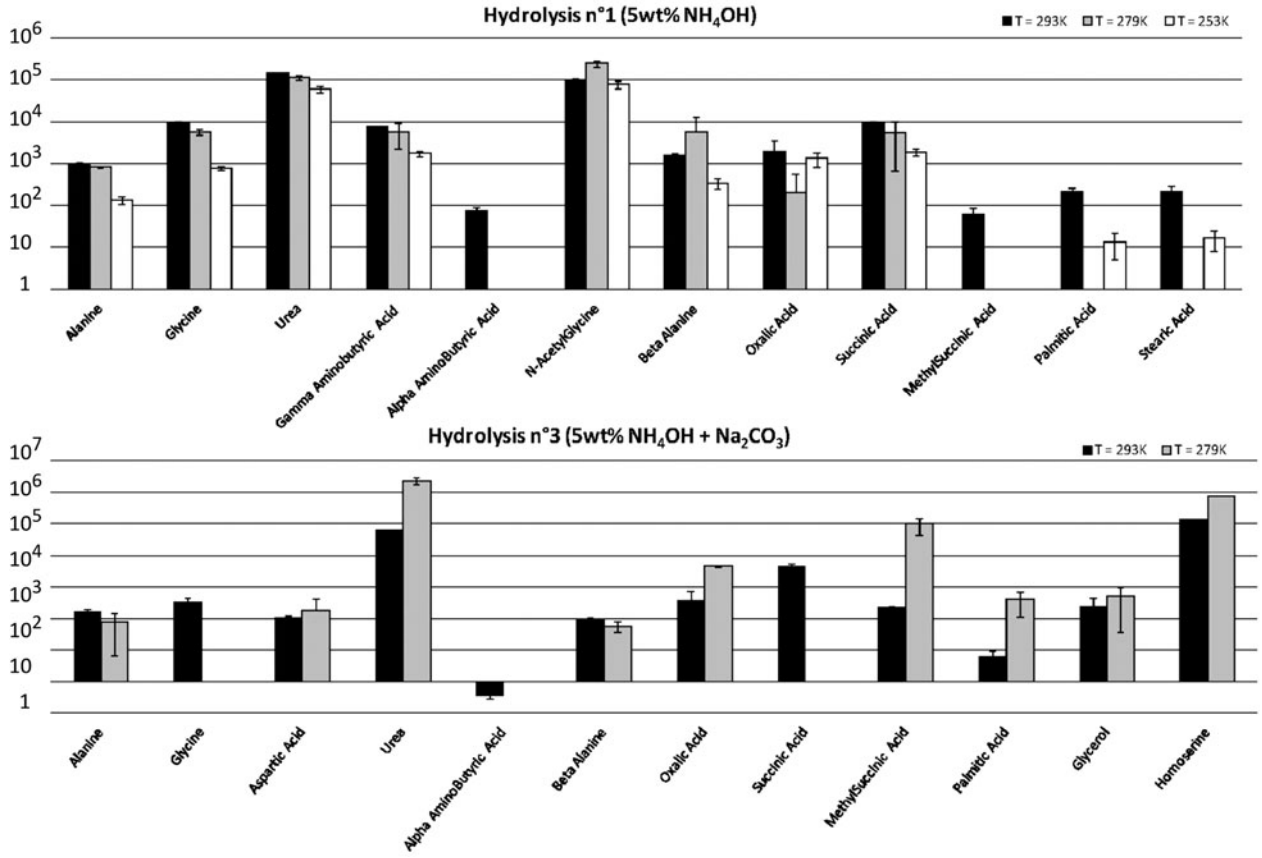

FIG. 5. Histograms presenting the production yields of detected organics by gas chromatography–mass spectrometry after free-oxygen tholin hydrolysis in a water-ammonia (5 wt %) mixture without (hydrolysis n°1—top) and with (hydrolysis n°3—bottom) carbonates. Yields have been multiplied by 10^6 for clarity.

stearic acid. For hydrolysis n°3, 13 products, though several are different from the previous list, were also identified: alanine, glycine, aspartic acid, urea, α-aminobutyric acid, β-alanine, oxalic acid, succinic acid, methylsuccinic acid, palmitic acid, glycerol, homoserine, and crotonic acid. Moreover, we can see that all production yields are lower in the presence of carbonates (hydrolysis n°3), except for urea at 279 K and methylsuccinic acid for both temperatures. Indeed, for hydrolysis n°1, the production yields range from 10^{-1}% to 10^{-3}%, while for hydrolysis n°3 it goes from 1% to 10^{-5}% for the compounds detected in both hydrolyses.

As can be seen in Fig. 5 and Table 8, some compounds are specific of a particular hydrolysis. Stearic acid, γ-aminobutyric acid, and *N*-acetylglycine are only produced in basic media (NH_3) without carbonates (hydrolysis n°1—black dashed box in Table 8 and Fig. 6). While aspartic acid, glycerol, homoserine, and crotonic acid are only produced in the presence of carbonates in a basic media (hydrolysis n°3—gray lined box in Table 8 and Fig. 6).

Table 8 and Fig. 5 show the influence of the temperature on the formation of the majority of the detected molecules. At low temperatures, glycine and succinic acid are not produced in the presence of carbonates, and on the contrary, methylsuccinic acid is not produced in the absence of carbonates. On the other hand, α-aminobutyric acid is not produced at low temperatures in the presence or absence of carbonates. This suggests that this compound cannot be formed at the surface of Titan considering its very low temperature (around 94 K).

In the absence of carbonates (hydrolysis n°1), for most of the compounds, there is a correlation between the hydrolysis temperature and the production yields of organics. For these compounds, the formation reaction is endothermic, endergonic, or both. On the contrary, in the presence of carbonates (hydrolysis n°3), for most compounds, when the hydrolysis temperature increases, the production yields of the hydrolysis products decrease. Thus in the presence of carbonates, for several compounds, the formation reaction becomes exothermic, exergonic, or both. Under the temperature range studied, alanine and β-alanine are an exception. Indeed, temperature does not seem to have any influence. Even though the temperature is not the only parameter impacting the rate of reaction, commonly when the evolution temperature increases, the rate of reaction increases, so the production yield increases. In the presence of carbonates, this is not the case, and we do not have an endothermic/endergonic reaction but an exothermic/exergonic one. This is why it is possible to assume that carbonates could involve another formation pathway.

3.2. Comparison with other works

Other teams have studied different hydrolysis conditions of Titan tholins:

Table 8. Recap of the Production Yields (x_{wt}) and the Standard Deviation (σ) of Alanine, Glycine, Urea, α-Aminobutyric Acid, γ-Aminobutyric Acid, *N*-Acetylglycine, β-Alanine, Aspartic Acid, Homoserine, Glycerol, Crotonic Acid, Oxalic Acid, Succinic Acid, Methylsuccinic Acid, Palmitic Acid, and Stearic Acid after Free-Oxygen Tholin Hydrolysis at Three Different Evolution Temperatures: 293, 279, and 259 K

	Hydrolysis n°1						Hydrolysis n°3			
	293K		279K		253K		293K		279K	
	x_{wt} (%)	σ (%)	x_{wt} (%)	σ (%)	x_{wt} (%)	σ (%)	x_{wt} (%)	σ (%)	x_{wt} (%)	σ (%)
Alanine	1.00E-01	5.08E-03	8.50E-02	4.44E-03	1.38E-02	2.89E-03	1.69E-02	3.00E-03	7.53E-03	6.83E-03
Glycine	9.20E-01	8.55E-02	5.79E-01	9.15E-02	7.93E-02	8.11E-03	3.42E-02	1.02E-02	ND	ND
Urea	1.44E+01	7.30E-01	1.14E+01	1.52E+00	6.10E+00	1.10E+00	6.23E+00	1.65E-01	2.32E+02	5.82E+01
Methylsuccinic acid	6.04E-03	2.83E-03	ND	ND	ND	ND	2.22E-02	1.44E-03	9.80E+00	5.44E+00
α-aminobutyric acid	7.54E-03	1.74E-03	ND	ND	ND	ND	3.59E-05	7.42E-06	ND	ND
Palmitic acid	2.16E-02	4.71E-03	ND	ND	1.34E-03	8.30E-04	6.30E-04	2.85E-04	4.06E-02	2.94E-02
β-Alanine	1.59E-01	1.64E-02	5.72E-01	7.15E-01	3.46E-02	8.95E-03	8.86E-03	2.27E-03	5.82E-03	2.04E-03
Oxalic acid	1.98E-01	1.47E-01	2.09E-02	3.61E-02	1.33E-01	4.82E-02	3.69E-02	3.45E-02	4.56E-01	3.42E-02
N-Acetylglycine	9.72E+00	1.27E+00	2.49E+01	4.15E+00	7.84E+00	1.61E+00	ND	ND	ND	ND
γ-aminobutyric acid	7.42E-01	2.16E-02	5.69E-01	3.43E-01	1.76E-01	2.80E-02	ND	ND	ND	ND
Stearic acid	2.12E-02	7.13E-03	ND	ND	1.68E-03	8.71E-04	ND	ND	ND	ND
Succinic acid	9.36E-01	9.01E-02	5.53E-01	4.85E-01	1.87E-01	3.58E-02	4.63E-01	8.92E-02	ND	ND
Aspartic acid	ND	ND	ND	ND	ND	ND	1.05E-02	1.40E-03	1.85E-02	2.21E-02
Glycerol	ND	ND	ND	ND	ND	ND	2.34E-02	2.14E-02	5.05E+02	4.66E-02
Homoserine	ND	ND	ND	ND	ND	ND	1.43E-01	1.61E+00	7.49E+01	3.36E+01
Crotonic acid	ND	ND	ND	ND	ND	ND	D	D	ND	ND

The black dashed box represents compounds only produced in basic media (NH_3) without carbonates (hydrolysis n°1). The gray lined box represents compounds only produced in the presence of carbonates in a basic media (hydrolysis n°3).

ND = not detected. D = detected but no quantification possible.

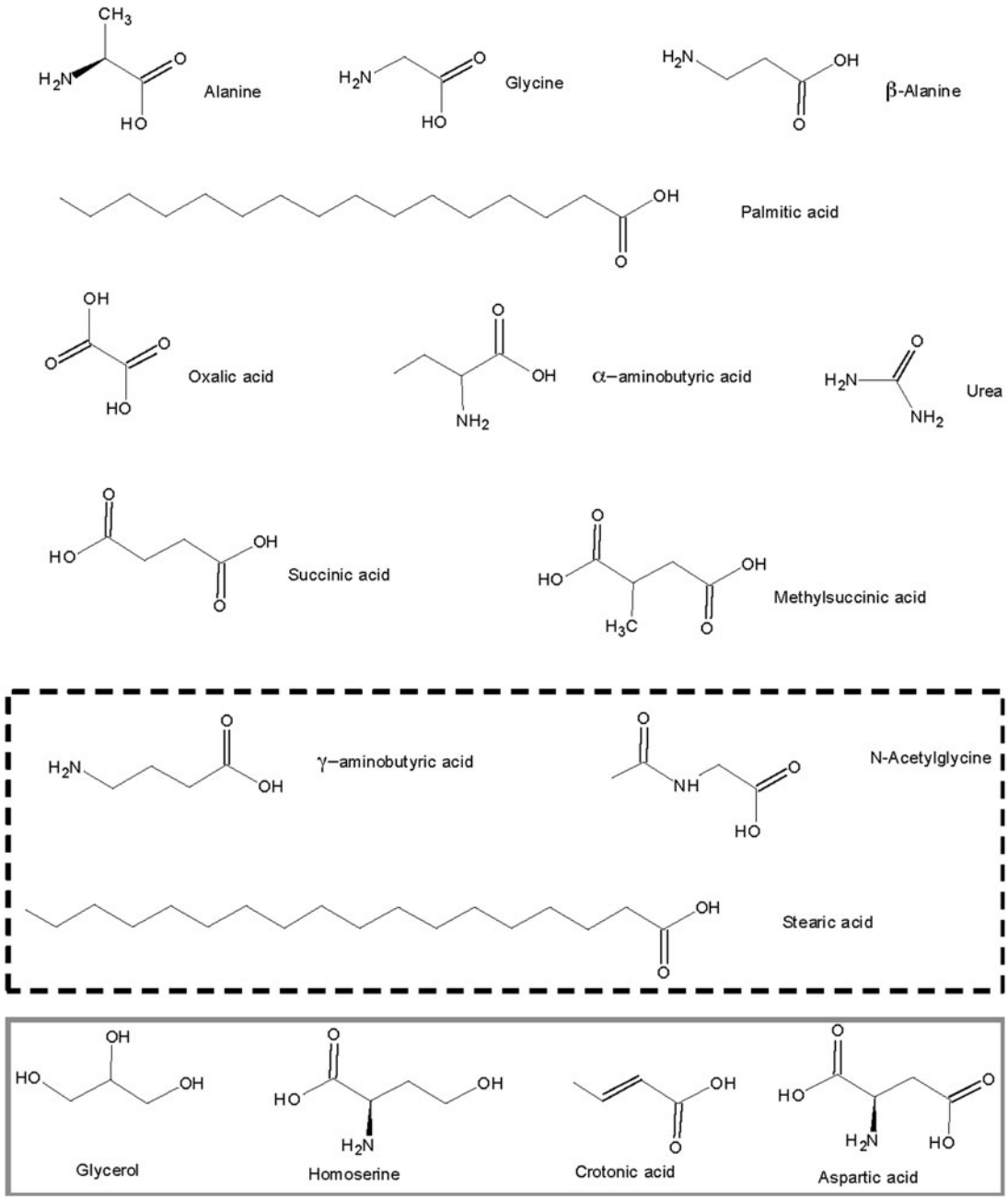

FIG. 6. Organics identified after the hydrolysis of free-oxygen tholins with or without carbonates. The black dashed box represents compounds only produced in basic media (NH_3) without carbonates (hydrolysis n°1). The gray lined box represents compounds only produced in the presence of carbonates (hydrolysis n°3).

- Acidic pH hydrolysis with hydrochloric acid (HCl) at 6 mol L^{-1} (Khare *et al.*, 1986; Nguyen, 2007; Taniuchi *et al.*, 2013) and at 2 mol L^{-1} (Nguyen, 2007).
- Neutral pH hydrolysis (pH = 7) (Nguyen, 2007).
- Alkaline pH hydrolysis with water-ammonia 25 wt % (Ramirez *et al.*, 2010; Poch *et al.*, 2012), 13 wt % (Neish *et al.*, 2009; Ramirez *et al.*, 2010), or 6.25 and 3.125 wt % (Ramirez *et al.*, 2010).

Table 9 sums up the qualitative identification results from both hydrolyses investigated in the present study and from other hydrolysis experiments cited above. These studies differ in their hydrolysis experimental conditions but also in the kind of Titan tholins used (produced by different experimental devices). However, in these works, the analytical techniques used were able to detect most of the hydrolysis products identified in the present study. Nevertheless, Neish *et al.* (2009) had a different purpose for their study that did not involve the identification of the hydrolysis products. This is why the results related to the work of Neish *et al.* (2009) are not reported in Table 9. Moreover, Poch *et al.* (2012) and Ramirez *et al.* (2010) conducted their studies on tholins synthesized with the experimental device PLASMA before its improvement to avoid air contamination, though they used the same general experimental conditions that were used in the present study. This is why

Table 9. Summary of the Hydrolysis Products of This Study and Other Studies Conducted with Different Experimental Conditions and on Different Kinds of Titan Tholins

	Hydrolysis n°1			Hydrolysis n°3		Khare et al. (1986)	Nguyen (2007)			Taniuchi et al. (2013)
	293K	279K	253K	293K	279K	HCl 6M 373K	HCL 6M 343K	HCL 2M 343K	pH 7 343K	HCl 6M 383K
Alanine	x	x	x	x	x	x	x	x	x	x
Glycine	x	x	x	x		x		x	x	x
Aspartic acid				x	x	x				x
Urea	x	x	x	x	x	x		x	x	
γ-aminobutyric acid	x	x	x			x				
α-aminobutyric acid	x			x		x	x	x	x	x
N-acetylglycine	x	x	x			x				
β-Alanine	x	x	x	x	x	x		x		x
Oxalic acid	x	x	x	x	x		x	x	x	
Succinic acid	x	x	x	x			x	x	x	
Methylsuccinic acid	x			x	x		x	x	x	
Palmitic acid	x		x	x	x					
Stearic acid	x		x							
Glycerol				x	x					
Homoserine				x	x					
Crotonic acid				x						

the results related to these authors' works are not reported in Table 9 as well.

Most of the compounds identified in our study have also been detected in other studies as displayed in Table 9. The production of alanine, glycine, urea, α-aminobutyric acid, γ-aminobutyric acid, *N*-acetylglycine, β-alanine, aspartic acid, oxalic acid, succinic acid, and methylsuccinic acid does not seem to be specific of the experimental conditions carried out in the present study. On the contrary, palmitic acid, stearic acid, homoserine, crotonic acid, and glycerol were identified for the first time after Titan tholin hydrolysis. Concerning palmitic acid, the latter is produced with or without carbonates, so it appears that carbonates do not impact their formation, while the water-ammonia (5 wt %) mixture does. However, glycerol, homoserine, and crotonic acid are produced only in the presence of carbonates (hydrolysis n°3). So it seems that the main factor in the formation of these three compounds might be the presence of carbonates, which reveals the noticeable carbonate impact on hydrolysis product.

4. Discussion

4.1. Astrobiological consequences

Previous studies on the hydrolysis of Titan's tholins have shown that they can react efficiently in alkaline solutions, even at low temperature, to produce complex organic compounds. The incorporation of O atoms provided by water molecules into the tholins appears faster in the presence of ammonia (Neish *et al.*, 2009), producing various molecules of biological interest, such as asparagine, aspartic acid, glutamine, and glutamic acid (Neish *et al.*, 2010). Ramirez *et al.* (2010) showed that the hydrolysis rate strongly decreases with temperature but that even at low temperatures a large variety of amino acids are still detectable. Similar results were obtained by Poch *et al.* (2012), who observed that the main product is urea. All these works suggest that alkaline pH hydrolysis of Titan's tholins plays a catalytic role in the formation of astrobiologically interesting compounds. The present study, using a smaller and realistic ammonia concentration, shows that the diversity of organic products, including compounds of astrobiological interest, can be largely enhanced by the presence of carbonates in the starting aqueous solution.

In all our experiments, urea was the main hydrolysis product both in the presence and absence of carbonates. Moreover, several amino acids, carboxylic acids, and fatty acids were produced as well. Three compounds were produced only when carbonates were present in the aqueous ammonia solution—glycerol, crotonic acid, and homoserine. These compounds are of astrobiological importance because of their potential role in prebiotic chemistry. Glycerol is the starting molecule toward glycerol monoacyl derivatives, which would have been important for prebiotic membranes (Maurer *et al.*, 2009). Crotonic acid is one of the simplest unsaturated fatty acids, which are components of lipids. Homoserine is one of the important nonprotein amino acids in prebiotic chemistry (Zaia *et al.*, 2008).

4.2. Possible chemical pathways

The production of some of the identified compounds can be explained by the chemical composition of tholins. Indeed,

understanding the chemical pathways responsible for the formation of hydrolysis product can give insights into the composition of tholins' soluble phase and, by extrapolation, of Titan aerosols' soluble phase. For example, urea could be synthesized from a carbodiimide group (-N=C=N-) via nucleophilic attack. It must be noticed that the presence of carbodiimide group in Titan tholins was suspected by Imanaka *et al.* (2004).

$$HN = C = NH + H_2O \rightarrow H_2N - CO - NH_2$$

Concerning the production of amino acids in an alkaline pH environment, the pathway most often considered is the Strecker reaction. But it begins with an oxygenated molecule, an aldehyde (RCHO), which cannot be available in the starting clean and O-free tholins. Thus, we must look for non-oxygenated precursors. Another chemical pathway was proposed by Poch *et al.* (2012), which involves the hydrolysis of the nitrile group (CN) of an aminonitrile ($RCH(NH_2)CN$) followed by the elimination of ammonia (NH_3) as detailed in Fig. 7. Nevertheless, it is also assumed that tholins could be constituted of heteropolymers that would induce a similar, though more complex, chemical pathway concerning the amino acids' production (Thompson and Sagan, 1989) involving the reduction of an imide group followed by a hydrolysis step.

For carboxylic acids (RCOOH), it is possible to apply the chemical pathway proposed for amino acid formation (Fig. 7), replacing the aminonitrile by a nitrile (RCN). The alcohol group, which is present for example in homoserine, can be obtained from the hydrolysis of an alkene (C=C). However, the presence of a carbon-carbon double bond within a molecule with a nitrile group could induce the production of several different molecules with an alcohol group. This shows that these chemical schemes must be considered very carefully.

These different chemical pathways suggest potential precursors that lead to the formation of the whole hydrolysis products in an alkaline pH environment as displayed in Table 10. This list contains mostly nitriles. This supports the idea that tholins could be made of HCN polymers or oligomers (Raulin, 2005, and references therein). Moreover, some of these potential precursors have already been identified in Titan tholins synthesized from CH_4/N_2 (5/95) such as aminoacetonitrile and butanedinitrile (He and Smith, 2014).

The list in Table 10 can be used as a database of target molecules or at least functional groups that can be identified in Titan tholins and—by extrapolation—in Titan aerosols by looking at the potential precursors. In this way, we could get some leads about the chemical composition of these particles. This kind of work is already the subject of many studies that use various analytical instruments such as UV spectroscopy, IR spectroscopy, UV fluorescence, elementary analysis, mass spectroscopy, pyrolysis gas chromatography and gas chromatography–mass spectrometry, and nuclear magnetic resonance spectroscopy. However, this rarely leads to the identification of the full molecular structure, except for new studies carried out with nuclear magnetic resonance spectroscopy on tholins (*e.g.*, He *et al.*, 2012; He and Smith, 2013, 2014).

4.3. Extrapolation to Titan

These hydrolysis experiments were conducted at temperatures between 293 and 253 K, while Titan's surface temperature is around 94 K. Could the identified compounds in this study be produced under Titan's surface conditions? Indeed, we can imagine that the chemical kinetics of all reactions leading to the formation of the compounds produced during those experiments would be much slower at

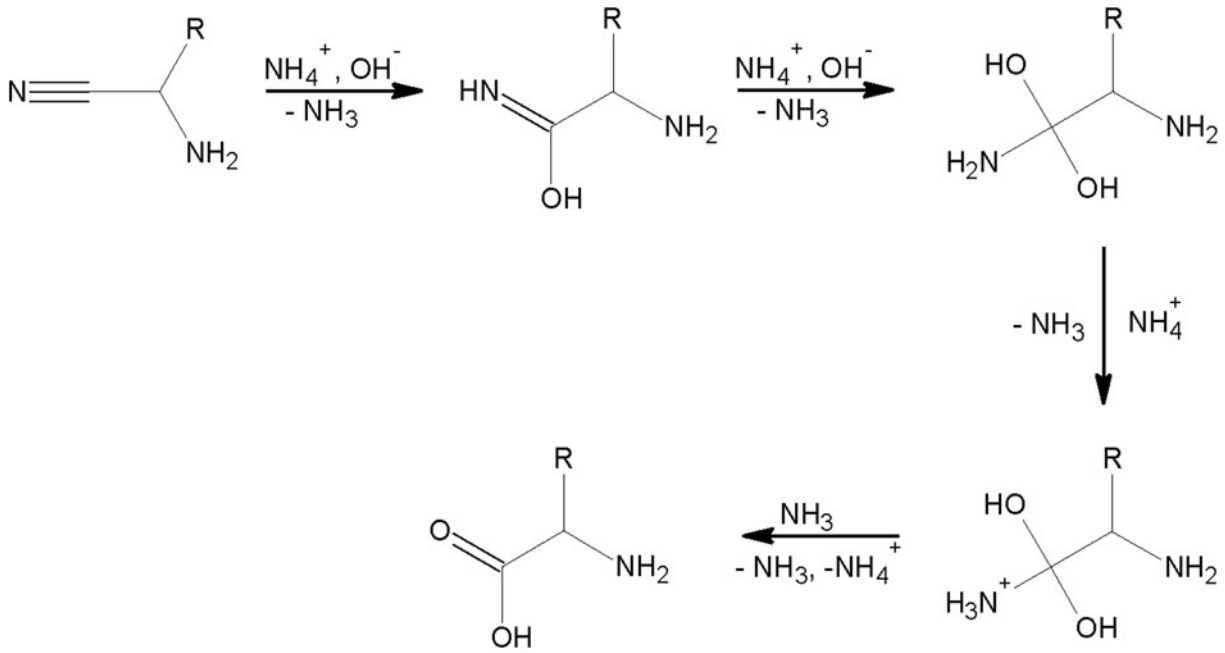

FIG. 7. A possible chemical pathway for the formation of amino acids via alkalino pH hydrolysis of Titan tholins. Adapted from Poch *et al.* (2012).

TABLE 10. POTENTIAL PRECURSORS THAT LEAD TO THE FORMATION OF THE WHOLE HYDROLYSIS PRODUCTS IDENTIFIED IN THIS STUDY

Hydrolysis products		Potential precursors	
Name	Semi structural formula	Name	Semi structural formula
Alanine	NH_2-CH(CH_3)-COOH	2-Aminopropionitrile	NH_2-CH(CH_3)-CN
Glycine	NH_2-CH_2-COOH	Aminoacetonitrile	NH_2-CH_2-CN
Urea	NH_2-CO-NH_2	Carbodiimide	NH=C=NH
Methylsuccinic acid	HOOC-CH(CH_3)-CH_2-COOH	2-Methylbutanedinitrile	NC-CH(CH_3)-CH_2-CN
α-aminobutyric acid	CH_3-CH_2-CH(NH_2)-COOH	2-Aminobutanenitrile	CH_3-CH_2-CH(NH_2)-CN
Palmitic acid	CH_3-$(CH_2)_{14}$-COOH	Hexadecanenitrile	CH_3-$(CH_2)_{14}$-CN ?
β-Alanine	NH_2-CH_2-CH_2-COOH	3-Aminopropanenitrile	NH_2-CH_2-CH_2-CN
Oxalic acid	HOOC-COOH	Oxalonitrile	NC-CN
Succinic acid	HOOC-CH_2-CH_2-COOH	Butanedinitrile	NC-CH_2-CH_2-CN
γ-aminobutyric acid	NH_2-CH_2-CH_2-CH_2-COOH	4-Aminobutanenitrile	NH_2-CH_2-CH_2-CH_2-CN
Stearic acid	CH_3-$(CH_2)_{16}$-COOH	Octadecanenitrile	CH_3-$(CH_2)_{16}$-CN ?
N-Acetylglycine	CH_3-CO-NH-CH_2-COOH	-	?
Aspartic acid	HOOC-CH(NH_2)-CH_2-COOH	2-Aminobutanedinitrile	NC-CH(NH_2)-CH_2-CN
Glycerol	$HOCH_2$-CH(OH)-CH_2OH	-	?
Homoserine	$HOCH_2$-CH_2-CH(NH_2)-COOH	2-Aminobut-3-enenitrile	CH_2=CH-CH(NH_2)-CN
Crotonic acid	CH_3-CH=CH-COOH	But-2-enenitrile	CH_3-CH=CH-CN

Titan's surface temperature, and the contribution of several reactions involved in their synthesis could be quite different. Nevertheless, although the results need to be considered with caution, Ramirez *et al.* (2010) conducted hydrolysis experiments on tholins at 96 K, which is close to Titan's surface temperature, and showed that some hydrolysis products can be detected at this low temperature. Consequently, it is reasonable to assume that some of the compounds of astrobiological interest characterized in this study could also be present at the surface of Titan if there is indeed cryovolcanic activity and by extension the presence of a water-ammonia mixture.

Thus, the list in Table 10 can also be used as a database of target molecules that can be searched for at the surface of Titan, in particular in potentially cryovolcanic areas by looking at the hydrolysis products. This is the case of Sotra Facula (Sotra Patera) and Hotei Regio (Lopes *et al.*, 2011, 2013), which are among the best candidates for cryovolcanism activity locations on Titan. Nevertheless, it is important to evaluate whether these compounds have a lifetime long enough under the satellite's surface conditions to be detected. This is why it would be necessary to carry out new experiments in order to study their potential lifetime at the surface of Titan, for example, by putting in place experiments of degradation of organic material, which will take into account the actual knowledge on energetic flux that reaches the surface. One of those energetic sources reaching the surface that could be simulated in the laboratory is cosmic rays. Recently, it has been suggested that Titan's internal ocean could be free of ammonia. Such a different composition could impact the nature and the diversity of hydrolysis products since it has been shown that hydrolysis of tholins is more efficient in the presence of ammonia than it is in pure water (Neish *et al.*, 2009; Ramirez *et al.*, 2010; Poch *et al.*, 2012).

Finally, as pointed out by C. McKay (personal communication), the approach that was followed in the present work would also be of interest for the processing of Titan's tholins in the high-alkaline medium of Enceladus' ocean (Glein *et al.*, 2015).

Acknowledgments

This study has been supported by grants (U27 & U45) from the French Space Agency (CNES). F. Raulin thanks ESA for its support as IDS of the Cassini-Huygens mission. The authors wish to thank Bernard Frouin for his help in the preparation of this manuscript, and the two referees for their contribution in improving the manuscript.

References

Barnes, J.W., Brown, R.H., Turtle, E.P., McEwen, A.S., Lorenz, R.D., Janssen, M., Schaller, E.L., Brown, M.E., Buratti, B.J., Sotin, C., Griffith, C., Clark, R., Perry, J., Fussner, S., Barbara, J., West, R., Elachi, C., Bouchez, A.H., Roe, H.G., Baines, K.H., Bellucci, G., Bibring, J.P., Capaccioni, F., Cerroni, P., Combes, M., Coradini, A., Cruikshank, D.P., Drossart, P., Formisano, V., Jaumann, R., Langevin, Y., Matson, D.L., McCord, T.B., Nicholson, P.D., and Sicardy, B. (2005) A 5-micron-bright spot on Titan: evidence for surface diversity. *Science* 310:92–95.

Barnes, J.W., Brown, R.H., Radebaugh, J., Buratti, B.J., Sotin, C., Le Mouelic, S., Rodriguez, S., Turtle, E.P., Perry, J., Clark, R., Baines, K.H., and Nicholson, P.D. (2006) Cassini observations of flow-like features in western Tui Regio, Titan. *Geophys Res Lett* 33, doi:10.1029/2006GL026843.

Béghin, C., Randriamboarison, O., Hamelin, M., Karkoschka, E., Sotin, C., Whitten, R.C., Berthelier, J.-J., Grard, R., and Simões, F. (2012) Analytic theory of Titan's Schumann resonance: constraints on ionospheric conductivity and buried water ocean. *Icarus* 218:1028–1042.

Buch, A., Glavin, D.P., Sternberg, R., Szopa, C., Rodier, C., Navarro-González, R., Raulin, F., Cabane, M., and Mahaffy, P.R. (2006) A new extraction technique for *in situ* analyses of amino and carboxylic acids on Mars by gas chromatography mass spectrometry. *Planet Space Sci* 54:1592–1599.

Buch, A., Sternberg, R., Szopa, C., Freissinet, C., Garnier, C., Bekri, E.J., Rodier, C., Navarro-Gonzalez, R., Raulin, F., Cabane, M., Stambouli, M., Glavin, D.P., and Mahaffy, P.R. (2009) Development of a gas chromatography compatible Sample Processing System (SPS) for the *in situ* analysis of refractory organic matter in martian soil: preliminary results. *Adv Space Res* 43:143–151.

Butler, J.N. (1998) *Ionic Equilibrium: Solubility and pH Calculations*, 1st ed., with a chapter by D.R. Cogley, Wiley, New York.

Coll, P., Coscia, D., Gazeau, M.-C., Guez, L., and Raulin, F. (1997) New planetary atmosphere simulations: application to the organic aerosols of Titan. *Adv Space Res* 19:1113–1119.

Coustenis, A., Salama, A., Lellouch, E., Encrenaz, T., Bjoraker, G.L., Samuelson, R.E., de Graauw, T., Feuchtgruber, H., and Kessler, M.F. (1998) Evidence for water vapor in Titan's atmosphere from ISO/SWS data. *Astron Astrophys* 336:L85–L89.

Coustenis, A., Jennings, D.E., Nixon, C.A., Achterberg, R.K., Lavvas, P., Vinatier, S., Teanby, N.A., Bjoraker, G.L., Carlson, R.C., Piani, L., Bampasidis, G., Flasar, F.M., and Romani, P.N. (2010) Titan trace gaseous composition from CIRS at the end of the Cassini–Huygens prime mission. *Icarus* 207:461–476.

Elachi, C., Wall, S., Allison, M., Anderson, Y., Boehmer, R., Callahan, P., Encrenaz, P., Flamini, E., Franceschetti, G., Gim, Y., Hamilton, G., Hensley, S., Janssen, M., Johnson, W., Kelleher, K., Kirk, R., Lopes, R., Lorenz, R., Lunine, J., Muhleman, D., Ostro, S., Paganelli, F., Picardi, G., Posa, F., Roth, L., Seu, R., Shaffer, S., Soderblom, L., Stiles, B., Stofan, E., Vetrella, S., West, R., Wood, C., Wye, L., and Zebker, H. (2005) Cassini radar views the surface of Titan. *Science* 308:970–974.

Flasar, F.M., Achterberg, R.K., Conrath, B.J., Gierasch, P.J., Kunde, V.G., Nixon, C.A., Bjoraker, G.L., Jennings, D.E., Romani, P.N., Simon-Miller, A.A., Bezard, B., Coustenis, A., Irwin, P.G.J., Teanby, N.A., Brasunas, J., Pearl, J.C., Segura, M.E., Carlson, R.C., Mamoutkine, A., Schinder, P.J., Barucci, A., Courtin, R., Fouchet, T., Gautier, D., Lellouch, E., Marten, A., Prange, R., Vinatier, S., Strobel, D.F., Calcutt, S.B., Read, P.L., Taylor, F.W., Bowles, N., Samuelson, R.E., Orton, G.S., Spilker, L.J., Owen, T.C., Spencer, J.R., Showalter, M.R., Ferrari, C., Abbas, M.M., Raulin, F., Edgington, S., Ade, P., and Wishnow, E.H. (2005) Titan's atmospheric temperatures, winds, and composition. *Science* 308:975–978.

Fortes, A.D. (2000) Exobiological implications of a possible ammonia-water ocean inside Titan. *Icarus* 146:444–452.

Glein, C.R., Baross, J.A., and Waite, J.H. (2015) The pH of Enceladus' ocean. *Geochim Cosmochim Acta* 162:202–219.

Grasset, O., Sotin, C., and Deschamps, F. (2000) On the internal structure and dynamics of Titan. *Planet Space Sci* 48:617–636.

Hayes, A., Aharonson, O., Wall, S., Sotin, C., LeGall, A., Lopes, R., Janssen, M., and the Cassini RADAR Team. (2008) Joint analysis of infrared and radar observations of Titan's surface using the Cassini VIMS and RADAR instruments. *Bulletin of the American Astronomical Society* 40:457.

He, C. and Smith, M.A. (2013) Identification of nitrogenous organic species in Titan aerosols analogs: nitrogen fixation routes in early atmospheres. *Icarus* 226:33–40.

He, C. and Smith, M.A. (2014) Identification of nitrogenous organic species in Titan aerosols analogs: implication for prebiotic chemistry on Titan and early Earth. *Icarus* 238:86–92.

He, C., Lin, G., and Smith, M.A. (2012) NMR identification of hexamethylenetetramine and its precursor in Titan tholins: implications for Titan prebiotic chemistry. *Icarus* 220:627–634.

Hersant, F., Gautier, D., and Lunine, J.I. (2004) Enrichment in volatiles in the giant planets of the Solar System. *Planet Space Sci* 52:623–641.

Hersant, F., Gautier, D., Tobie, G., and Lunine, J.I. (2008) Interpretation of the carbon abundance in Saturn measured by Cassini. *Planet Space Sci* 56:1103–1111.

Imanaka, H., Khare, B.N., Elsila, J.E., Bakes, E.L.O., McKay, C.P., Cruikshank, D.P., Sugita, S., Matsui, T., and Zare, R.N. (2004) Laboratory experiments of Titan tholin formed in cold plasma at various pressures: implications for nitrogen-containing polycyclic aromatic compounds in Titan haze. *Icarus* 168:344–366.

Khare, B.N., Sagan, C., Ogino, H., Nagy, B., Er, C., Schram, K.H., and Arakawa, E.T. (1986) Amino-acids derived from Titan tholins. *Icarus* 68:176–184.

Kirk, R., Howington-Kraus, E., Redding, B.L., Becker, T.L., Lee, E.M., Stiles, B.W., Hensley, S., and the Cassini RADAR Team. (2008) A three-dimensional view of Titan's surface features from Cassini RADAR stereogrammetry [abstract #P11D-09]. In *AGU 2008 Fall Meeting*, American Geophysical Union, Washington, DC.

Lide, D.R., editor-in-chief. (2006) *CRC Handbook of Chemistry and Physics*, 87th ed., CRC Press, Boca Raton, FL.

Lopes, R.M.C., Mitchell, K.L., Stofan, E.R., Lunine, J.I., Lorenz, R., Paganelli, F., Kirk, R.L., Wood, C.A., Wall, S.D., Robshaw, L.E., Fortes, A.D., Neish, C.D., Radebaugh, J., Reffet, E., Ostro, S.J., Elachi, C., Allison, M.D., Anderson, Y., Boehmer, R., Boubin, G., Callahan, P., Encrenaz, P., Flamini, E., Francescetti, G., Gim, Y., Hamilton, G., Hensley, S., Janssen, M.A., Johnson, W.T.K., Kelleher, K., Muhleman, D.O., Ori, G., Orosei, R., Picardi, G., Posa, F., Roth, L.E., Seu, R., Shaffer, S., Soderblom, L.A., Stiles, B., Vetrella, S., West, R.D., Wye, L., and Zebker, H.A. (2007) Cryovolcanic features on Titan's surface as revealed by the Cassini Titan Radar Mapper. *Icarus* 186:395–412.

Lopes, R.M.C., Stofan, E.R., Peckyno, R., Radebaugh, J., Mitchell, K.L., Mitri, G., Wood, C.A., Kirk, R.L., Wall, S.D., Lunine, J.I., Hayes, A., Lorenz, R., Farr, T., Wye, L., Craig, J., Ollerenshaw, R.J., Janssen, M., LeGall, A., Paganelli, F., West, R., Stiles, B., Callahan, P., Anderson, Y., Valora, P., and Soderblom, L. (2010) Distribution and interplay of geologic processes on Titan from Cassini radar data. *Icarus* 205:540–558.

Lopes, R.M.C., Kirk, R., Mitchell, K., LeGall, A., Stofan, E., Barnes, J., Kargel, J., Janssen, M., Hayes, A., Radebaugh, J., Wall, S., and the Cassini RADAR Team. (2011) Cryovolcanism on Titan: a re-assessment in light of new data from Cassini RADAR and VIMS [EPSC-DPS2011-303]. In *EPSC-DPS Joint Meeting 2011*, Vol. 6, European Planetary Science Congress and Division for Planetary Sciences of the American Astronomical Society.

Lopes, R.M.C., Kirk, R.L., Mitchell, K.L., LeGall, A., Barnes, J.W., Hayes, A., Kargel, J., Wye, L., Radebaugh, J., Stofan, E.R., Janssen, M.A., Neish, C.D., Wall, S.D., Wood, C.A., Lunine, J.I., and Malaska, M.J. (2013) Cryovolcanism on Titan: new results from Cassini RADAR and VIMS. *J Geophys Res: Planets* 118:416–435.

Lorenz, R.D. (1993) The surface of Titan in the context of ESA Huygens probe. *ESA Journal* 17:275–292.

Lorenz, R.D. and Lunine, J.I. (1996) Erosion on Titan: past and present. *Icarus* 122:79–91.

Lorenz, R.D., Stiles, B.W., Kirk, R.L., Allison, M.D., del Marmo, P.P., Iess, L., Lunine, J.I., Ostro, S.J., and Hensley, S. (2008) Titan's rotation reveals an internal ocean and changing zonal winds. *Science* 319:1649–1651.

Marten, A., Hidayat, T., Biraud, Y., and Moreno, R. (2002) New millimeter heterodyne observations of Titan: vertical distributions of nitriles HCN, HC_3N, CH_3CN, and the isotopic ratio $^{15}N/^{14}N$ in its atmosphere. *Icarus* 158:532–544.

Maurer, S.E., Deamer, D.W., Boncella, J.M., and Monnard, P.A. (2009) Chemical evolution of amphiphiles: glycerol monoacyl derivatives stabilize plausible prebiotic membranes. *Astrobiology* 9:979–987.

McCord, T.B., Hansen, G.B., Buratti, B.J., Clark, R.N., Cruikshank, D.P., D'Aversa, E., Griffith, C.A., Baines, E.K.H., Brown, R.H., Dalle Ore, C.M., Filacchione, G., Formisano, V., Hibbitts, C.A., Jaumann, R., Lunine, J.I., Nelson, R.M., Sotin, C., and the Cassini VIMS Team. (2006) Composition of Titan's surface from Cassini VIMS. *Planet Space Sci* 54:1524–1539.

McKay, C.P., Pollack, J.B., and Courtin, R. (1989) The thermal structure of Titan's atmosphere. *Icarus* 80:23–53.

McKay, C.P., Pollack, J.B., and Courtin, R. (1991) The greenhouse and antigreenhouse effects on Titan. *Science* 253:1118–1121.

Mitri, G., Showman, A.P., Lunine, J.I., and Lopes, R.M.C. (2008) Resurfacing of Titan by ammonia-water cryomagma. *Icarus* 196:216–224.

Mitri, G., Meriggiola, R., Hayes, A., Lefevre, A., Tobie, G., Genova, A., Lunine, J.I., and Zebker, H. (2014) Shape, topography, gravity anomalies and tidal deformation of Titan. *Icarus* 236:169–177.

Neish, C.D., Somogyi, A., and Smith, M.A. (2009) Low temperature hydrolysis of laboratory tholins in ammonia-water solutions: implications for prebiotic chemistry on Titan. *Icarus* 201:412–421.

Neish, C.D., Somogyi, A, Lunine, J.I., and Smith, M.A. (2010) Titan's primordial soup: formation of amino acids via low-temperature hydrolysis of tholins. *Astrobiology* 10:337–347.

Nelson, R.M., Kamp, L.W., Lopes, R.M.C., Matson, D.L., Kirk, R.L., Hapke, B.W., Wall, S.D., Boryta, M.D., Leader, F.E., Smythe, W.D., Mitchell, K.L., Baines, K.H., Jaumann, R., Sotin, C., Clark, R.N., Cruikshank, D.P., Drossart, P., Lunine, J.I., Combes, M., Bellucci, G., Bibring, J.-P., Capaccioni, F., Cerroni, P., Coradini, A., Formisano, V., Filacchione, G., Langevin, Y., McCord, T.B., Mennella, V., Nicholson, P.D., Sicardy, B., Irwin, P.G.J., and Pearl, J.C. (2009) Photometric changes on Saturn's Titan: evidence for active cryovolcanism. *Geophys Res Lett* 36, doi:10.1029/2008GL036206.

Nguyen, M.J. (2007) Nouvelles contraintes sur la nature physico-chimique des aérosols de Titan: analyse des données de la mission Cassini-Huygens et simulation expérimentale en laboratoire. PhD thesis, Université Paris 12 Val-de-Marne, Créteil, France.

Niemann, H.B., Atreya, S.K., Bauer, S.J., Carignan, G.R., Demick, J.E., Frost, R.L., Gautier, D., Haberman, J.A., Harpold, D.N., Hunten, D.M., Israel, G., Lunine, J.I., Kasprzak, W.T., Owen, T.C., Paulkovich, M., Raulin, F., Raaen, E., and Way, S.H. (2005) The abundances of constituents of Titan's atmosphere from the GCMS instrument on the Huygens probe. *Nature* 438:779–784.

Niemann, H.B., Atreya, S.K., Demick, J.E., Gautier, D., Haberman, J.A., Harpold, D.N., Kasprzak, W.T., Lunine, J.I., Owen, T.C., and Raulin, F. (2010) Composition of Titan's lower atmosphere and simple surface volatiles as measured by the Cassini-Huygens probe gas chromatograph mass spectrometer experiment. *J Geophys Res: Planets* 115, doi:10.1029/2010JE003659.

Nixon, C.A., Jennings, D.E., Bézard, B., Vinatier, S., Teanby, N.A., Suug, K., Ansty, T.M., Irwin, P.G.J., Gorius, N., Coustenis, A., and Flasar, F.M. (2013) Detection of propene in Titan's stratosphere. *Astrophys J* 776, doi:10.1088/2041-8205/776/1/L14.

Poch, O., Coll, P., Buch, A., Ramirez, S.I., and Raulin, F. (2012) Production yields of organics of astrobiological interest from H_2O-NH_3 hydrolysis of Titan's tholins. *Planet Space Sci* 61:114–123.

Ramirez, S.I., Coll, P., Buch, A., Brasse, C., Poch, O., and Raulin, F. (2010) The fate of aerosols on the surface of Titan. *Faraday Discuss* 147:419–427.

Raulin, F. (2005) Exo-astrobiological aspects of Europa and Titan: from observations to speculations. *Space Sci Rev* 116: 471–487.

Raulin, F., Brasse, C., Poch, O., and Coll, P. (2012) Prebiotic-like chemistry on Titan. *Chem Soc Rev* 41:5380–5393.

Samuelson, R.E., Maguire, W.C., Hanel, R.A., Kunde, V.G., Jennings, D.E., Yung, Y.L., and Aikin, A.C. (1983) CO_2 on Titan. *J Geophys Res: Space Physics* 88:8709–8715.

Samuelson, R.E., Mayo, L.A., Knuckles, M.A., and Khanna, R.J. (1997) C_4N_2 ice in Titan's north solar stratosphere. *Planet Space Sci* 45:941–948.

Soderblom, L.A., Brown, R.H., Soderblom, J.M., Barnes, J.W., Kirk, R.L., Sotin, C., Jaumann, R., Mackinnon, D.J., Mackowski, D.W., Baines, K.H., Buratti, B.J., Clark, R.N., and Nicholson, P.D. (2009) The geology of Hotei Regio, Titan: correlation of Cassini VIMS and RADAR. *Icarus* 204:610–618.

Sotin, C., Jaumann, R., Buratti, B.J., Brown, R.H., Clark, R.N., Soderblom, L.A., Baines, K.H., Bellucci, G., Bibring, J.P., Capaccioni, F., Cerroni, P., Combes, M., Coradini, A., Cruikshank, D.P., Drossart, P., Formisano, V., Langevin, Y., Matson, D.L., McCord, T.B., Nelson, R.M., Nicholson, P.D., Sicardy, B., LeMouelic, S., Rodriguez, S., Stephan, K., and Scholz, C.K. (2005) Release of volatiles from a possible cryovolcano from near-infrared imaging of Titan. *Nature* 435:786–789.

Sotin, C., Brown, R.H., Lawrence, K., Le Mouélic, S., Barnes, J., Soderblom, J., and the VIMS Team. (2010) High resolution mapping of Titan with VIMS. In *European Planetary Science Congress 2010*, EPSC, Rome, p 856.

Stiles, B.W., Hensley, S., Gim, Y., Bates, D.M., Kirk, R.L., Hayes, A., Radebaugh, J., Lorenz, R.D., Mitchell, K.L., Callahan, P.S., Zebker, H., Johnson, W.T.K., Wall, S.D., Lunine, J.I., Wood, C.A., Janssen, M., Pelletier, F., West, R.D., and Veeramacheneni, C. (2009) Determining Titan surface topography from Cassini SAR data. *Icarus* 202:584–598.

Taniuchi, T., Takano, Y., and Kobayashet, K. (2013) Amino acid precursors from a simulated lower atmosphere of Titan: experiments of cosmic ray energy source with C-13- and O-18-stable isotope probing mass spectrometry. *Anal Sci* 29: 777–785.

Thompson, W.R. and Sagan, C. (1989) Atmospheric formation of organic heteropolymers from N_2+CH_4: structural suggestions for amino acid and oligomer precursors. *Orig Life Evol Biosph* 19:503–504.

Tobie, G., Grasset, O., Lunine, J.I., Mocquet, A., and Sotin, C. (2005) Titan's internal structure inferred from a coupled thermal-orbital model. *Icarus* 175:496–502.

Tobie, G., Lunine, J.I., and Sotin, C. (2006) Episodic outgassing as the origin of atmospheric methane on Titan. *Nature* 440:61–64.

Tobie, G., Gautier, D., and Hersant, F. (2012) Titan's bulk composition constrained by Cassini-Huygens: implication for internal outgassing. *Astrophys J* 752, doi:10.1088/0004-637X/752/2/125.

Waite, J.H., Jr., Niemann, H., Yelle, R.V., Kasprzak, W.T., Cravens, T.E., Luhmann, J.G., McNutt, R.L., Ip, W.-H., Gell, D., De La Haye, V., Müller-Wordag, I., Magee, B., Borggren, N., Ledvina, S., Fletcher, G., Walter, E., Miller, R., Scherer, S., Thorpe, R., Xu, J., Block, B., and Arnett, K. (2005) Ion neutral mass spectrometer results from the first flyby of Titan. *Science* 308:982–986.

Waite, J.H., Jr., Young, D.T., Cravens, T.E., Coates, A.J., Crary, F.J., Magee, B., and Westlake, J. (2007) The process of tholin formation in Titan's upper atmosphere. *Science* 316:870–875.

Wall, S.D., Lopes, R.M., Stofan, E.R., Wood, C.A., Radebaugh, J.L., Hörst, S.M., Stiles, B.W., Nelson, R.M., Kamp, L.W., Janssen, M.A., Lorenz, R.D., Lunine, J.I., Farr, T.G., Mitri, G., Paillou, P., Paganelli, F., and Mitchell, K.L. (2009) Cassini RADAR images at Hotei Arcus and western Xanadu, Titan: evidence for geologically recent cryovolcanic activity. *Geophys Res Lett* 36, doi:10.1029/2008GL036415.

Zaia, D.A.M., Zaia, C.T.B.V., and De Santana, H. (2008) Which amino acids should be used in prebiotic chemistry studies? *Orig Life Evol Biosph* 38:469–488.

Address correspondence to:
François Raulin
Laboratoire Interuniversitaire des Systèmes Atmosphériques (LISA)
UMR CNRS 7583
Université Paris Est Créteil et Université Paris Diderot
Institut Pierre Simon Laplace, C.M.C.
61 avenue du Général de Gaulle
94010 Créteil Cédex
France

E-mail: francois.raulin@lisa.u-pec.fr

Submitted 3 May 2016
Accepted 4 August 2016

Abbreviations Used

DMF = dimethylformamide
GC = gas chromatograph
MS = mass spectrometer
MTBSTFA = *N*-methyl-*N*-(*tert*-butyldimethylsilyl)-trifluoroacetamide
SAR = Synthetic Aperture Radar
VIMS = Visual and Infrared Mapping Spectrometer